The CorC proteins MgpA (YoaE) and CorC protect from excess-cation stress and are required for egg white tolerance and virulence in *Salmonella*

Yumi Iwadate[1], and James M. Slauch[1*]

[1]Department of Microbiology, University of Illinois at Urbana-Champaign, Urbana, IL, 61801, USA.

*Correspondence: James M. Slauch
Department of Microbiology
University of Illinois
B103 CLSL, MC-110
601 S Goodwin Ave
Urbana, IL 61801
217-244-1956
slauch@illinois.edu

Running title: CorC and MgpA protect from excess-cation stress

Keywords: Magnesium, Polyamines, *Salmonella*, Cations, Stationary Phase, Egg White

ABSTRACT 250 words

Cation homeostasis is a vital function. In *Salmonella*, growth in very low Mg^{2+} induces expression of high-affinity Mg^{2+} transporters and synthesis of polyamines, organic cations that substitute for Mg^{2+}. Once Mg^{2+} levels are re-established, the polyamines must be excreted by PaeA. Otherwise, cells lose viability due to a condition we term excess-cation stress. We sought additional tolerance mechanisms for this stress. We show that CorC and MgpA (YoaE) are essential for survival in stationary phase after Mg^{2+} starvation. Deletion of *corC* causes a loss of viability additive with the *paeA* phenotype. Deletion of *mgpA* causes a synthetic defect in the *corC* background. This lethality is suppressed by loss of the inducible Mg^{2+} transporters, suggesting that the *corC mgpA* mutant is sensitive to changes in intracellular Mg^{2+}. CorC and MgpA function independently of PaeA. A *paeA* mutant is sensitive to externally added polyamine in stationary phase; loss of CorC and MgpA suppressed this sensitivity. Conversely, the *corC mgpA* mutant, but not the *paeA* mutant, exhibited sensitivity to high Mg^{2+} and egg white. The *corC mgpA* mutant is also attenuated in a mouse model. The *corC* and *mgpA* genes are induced in response to increased Mg^{2+} concentrations. Thus, CorC and MgpA play some interrelated role in cation homeostasis. It is unlikely that these phenotypes are due to absolute levels of cations. Rather, the cell maintains relative concentrations of various cations that likely compete for binding to anionic components. Imbalance of these cations affects some essential function(s), leading to a loss of viability.

IMPORTANCE

Mg^{2+} and other cations are critical for counteracting anionic compounds in the cell including RNA, DNA, and nucleotides. Both excessively low and high cation levels are toxic. To maintain proper intracellular concentrations, cells must regulate Mg^{2+} importers and exporters, or modulate the levels of other cations or anions that affect free Mg^{2+} levels. In *Salmonella*, no mutants sensitive to high Mg^{2+} levels have been identified. Here, we demonstrate that the largely uncharacterized proteins MgpA and CorC are induced under high Mg^{2+} conditions and are essential for tolerance to high Mg^{2+} levels. These genes are also essential for survival during endogenous excess-cation stress triggered by the transition to stationary phase after Mg^{2+} starvation, as well as for virulence, highlighting the broader role of cation homeostasis.

INTRODUCTION

Cations, particularly magnesium (Mg^{2+}), are required to stabilize RNA and DNA (1-3), counteract the negative charges on ATP (4), and neutralize the negative charges in outer membrane lipopolysaccharide (LPS) (5). Mg^{2+} is also critical for ribosome assembly, function, and stability (4, 6). Polyamines are organic cations important in all domains of life, but their physiological role is not well understood. Our recent data support a new paradigm for the overall role of polyamines in cell physiology. Our primary hypothesis is that polyamine and Mg^{2+} concentrations are coordinately controlled in the cell and that polyamines act as simple cations that can substitute for Mg^{2+} in critical systems under low-Mg^{2+} stress.

Salmonella Typhimurium is a major food-borne pathogen that replicates within macrophages, and adaptation to the low Mg^{2+} environment of the macrophage phagosome is key to *Salmonella* virulence. Counterintuitively, shifting *Salmonella* cells to Mg^{2+} deplete conditions induces an ultimate overload of cations that can be lethal upon reaching stationary phase. Upon Mg^{2+} starvation, polyamine synthesis is induced (7, 8), as is production of high affinity Mg^{2+} transporters MgtA and MgtB (9-13). Either polyamine synthesis or Mg^{2+} transport is required to maintain viability under these low Mg^{2+} conditions. Once Mg^{2+} levels are re-established, the excess polyamines must be excreted by the inner membrane polyamine exporter PaeA (7, 14). Mutants lacking PaeA lose viability when cells reach stationary phase. The lethality of the *paeA* mutant in stationary phase is suppressed by blocking Mg^{2+} transport, indicating that it is the total concentration of Mg^{2+} and polyamines that is detrimental, a phenomenon that we term "excess-cation stress." Importantly, these results are recapitulated during infection. Polyamine synthesis mutants are attenuated in a mouse model of systemic infection, as are strains lacking the MgtB Mg^{2+} transporter. Combined, these mutations confer a synthetic phenotype in animals, confirming that Mg^{2+} and polyamines are required for the same overall processes. These data support our hypothesis that the cell coordinately controls polyamine and Mg^{2+} concentrations to maintain overall cation homeostasis.

We sought additional proteins involved in mitigating excess-cation stress in *Salmonella*. We focused on the domain structure of the PaeA protein, particularly its C-terminal CorC domain. The PaeA protein contains an N-terminal transmembrane CNNM domain (pfam01595), and a cytoplasmic portion containing a CBS pair domain (pfam00571), followed by the C-terminal CorC_HlyC domain (pfam03471). The *Salmonella* genome encodes five additional proteins with CorC domains: CorB, CorC, MgpA (YoaE), YegH, and CvrA (Fig 1). CorB resembles PaeA with a CNNM transmembrane domain, CBS pair, and C-terminal CorC domain. The eponymous CorC lacks a transmembrane domain and has only a CBS pair

60 and C-terminal CorC domain. MgpA and YegH each possess an N-terminal transmembrane TerC domain
61 (pfam03741) followed by a CBS pair and C-terminal CorC domain. The CvrA protein contains an N-
62 terminal transmembrane Na/H^+ exchanger domain (pfam00999), and a cytoplasmic RCK domain
63 (pfam02080), followed by a CorC domain.

64 Although widespread, the biological and biochemical function of the CorC domain remains
65 unknown. We postulate that the CorC domain or the CBS pair/CorC domains function as a sensor of
66 cytoplasmic cations, such as Mg^{2+}. For example, our model suggests that PaeA exports polyamines in
67 response to the Mg^{2+} concentration (7). Moreover, all characterized CorC domain-containing proteins
68 appear to be involved in cation transport. PaeA in *Salmonella* and *E. coli* is responsible for the efflux of
69 cadaverine and putrescine (14). CorC and CorB were originally identified as conferring resistance to
70 cobalt in the medium and were further implicated in Mg^{2+} efflux (15). CorB homologs in the thermophilic
71 archaeon *Methanoculleus thermophilus* and the thermophilic Gram-negative bacterium *Tepidiphilus*
72 *thermophilus* are well-characterized Mg^{2+} efflux transporters (16, 17). In *Staphylococcus aureus*, the
73 CorB homolog, MpfA, is essential for tolerance to high Mg^{2+} levels (18). The CvrA protein in *Vibrio*
74 *cholerae* facilitates K^+/H^+ exchange (19). Collectively, these reports suggest that CorC domain-containing
75 proteins are crucial for maintaining proper cation levels and relative composition.

76 Given these findings, we examined whether any of the CorC domain-containing proteins in
77 *Salmonella* play a critical role in reducing excess-cation stress. Our results show that two of these
78 proteins, CorC and MgpA (YoaE), are required for full survival during stationary phase after Mg^{2+}
79 starvation, for full virulence in a mouse model, and for tolerance to high Mg^{2+} stress. (We have renamed
80 *yoaE* to *mgpA* for Mg^{2+} protection protein A). Thus, both CorC and MgpA play roles in mitigating excess-
81 cation stress, whether it arises endogenously or exogenously. Moreover, CorC and MgpA are required
82 for egg white tolerance, suggesting that exposure to egg white imposes cation imbalance in *Salmonella*.
83 The constitutive Mg^{2+} transporter CorA, previously believed to genetically interact with CorC (15), is
84 dispensable for CorC's role in survival during stationary phase after Mg^{2+} starvation, showing that CorC
85 functions independently of CorA. Our findings reveal that multilayered systems involving CorC domain-
86 containing proteins maintain proper cation levels in response to environmental changes, including during
87 host infection.
88
89

90 **RESULTS**

91 ***CorC is required for full survival under excess-cation stress in stationary phase.*** Our previous
92 studies revealed that, upon Mg^{2+} starvation, *Salmonella* induces both polyamine synthesis and high
93 affinity Mg^{2+} transport. Once Mg^{2+} levels are restored, PaeA is responsible for the efflux of the polyamines
94 cadaverine and putrescine. In the absence of PaeA, cells start to die upon entry into stationary phase (7,
95 14). We seek to further understand this excess-cation stress in stationary phase.

96 The C-terminus of PaeA contains a CorC domain. To better understand the CorC domain, we
97 initially focused on the eponymous CorC protein and investigated its role in response to induction of
98 excess-cation stress. The wild-type and Δ*corC* strains were grown in N-minimal medium (pH 7.4) with or
99 without Mg^{2+} at 37℃, and viability and OD_{600} were monitored for 48 hours. The Δ*corC* strain displayed a
100 decline in viability upon entry into stationary phase after Mg^{2+} starvation (Fig 2A). The OD_{600} was
101 unaffected in the Δ*corC* strain compared to the wild type grown in no Mg^{2+}, showing that the cells were
102 not lysing (Fig S1A). The *corC* gene is transcribed in an operon with upstream genes *ybeZ* and *ybeY* and
103 downstream gene, *Int* (20-22). To confirm that the phenotype results from loss of CorC, we introduced
104 low-copy number plasmids pWKS30 (vector) or pWKS30-*corC* into the Δ*corC* strain and examined
105 viability after Mg^{2+} starvation. As shown in Figure S2A, the phenotype of the Δ*corC* strain was fully
106 complemented by pWKS30-*corC*. These results suggest that CorC has an important role in maintaining
107 viability in stationary phase after Mg^{2+} starvation, similar to PaeA.

108 **Loss of CorC and MgpA confers synthetic phenotypes.** CorC is predicted to be a
109 cytoplasmic protein with no transmembrane domain, suggesting that CorC is not a transporter per se. To
110 investigate the mechanisms underlying the role of CorC in maintaining survival in stationary phase after
111 Mg^{2+} starvation, we asked if there was any genetic interaction between CorC and other CorC domain-
112 containing proteins. As we reported previously (7), a Δ*paeA* strain showed a loss of viability in stationary
113 phase after Mg^{2+} starvation (Fig. 2B). The deletion of the *corC* gene in the Δ*paeA* background further
114 decreased viability in stationary phase, with the results suggesting an apparent additive effect in the
115 double mutant (compare Fig. 2A and B). This suggests that *paeA* and *corC* are independently involved
116 in the same phenomenon, in a broad sense.

117 Deletion of *mgpA* had no apparent effect in stationary phase after Mg^{2+} starvation. However,
118 deletion of *mgpA* in the *corC* background notably intensified the loss of viability upon transition to
119 stationary phase after Mg^{2+} starvation (Fig. 2A). This suggests a synthetic relationship between the *mgpA*
120 and *corC* genes. In contrast to *mgpA*, deletion of the remaining CorC domain-containing proteins, *corB,*

121 *yegH, or cvrA*, conferred no apparent phenotype in either the wild-type or Δ*corC* backgrounds (Fig. S3),
122 indicating that they are not involved in this CorC-related phenomena under these conditions. Note that
123 YegH has the same general domain structure as MgpA (Fig. 1).

124 Introducing the pWKS30-*corC* plasmid into the Δ*mgpA* Δ*corC* strain restored viability in the
125 stationary phase, while a pWKS30-*mgpA* plasmid restored the phenotype to that of the Δ*corC* strain (Fig.
126 S2B). StyR-291, a sRNA encoded downstream of *mgpA* and antisense to the 3'- terminus of the *pdeD*
127 gene (23), does not affect the phenotype; a Δ*mgpA* Δ*corC* strain harboring the pWKS30-*mgpA*- StyR-
128 291 plasmid showed the same level of suppression of the strain harboring pWKS30-*mgpA* (Fig. S2B).
129 Deleting *mgpA* had no phenotypic effect in the Δ*paeA* strain, showing that there is no genetic interaction
130 between *mgpA* and *paeA* (Fig. 2B). The Δ*mgpA* mutation did exacerbate the phenotype seen in the Δ*corC*
131 Δ*paeA* background, as expected (Fig. 2B).

132 ***CorC and MgpA are required for survival when Mg^{2+} is imported.*** The lethality conferred by
133 loss of PaeA after Mg^{2+} starvation can be suppressed by loss of MgtA and MgtB Mg^{2+} transporters or by
134 blocking polyamine synthesis (Δsynth) (7). To gain further insight into the phenotypes of *mgpA* and *corC*
135 mutants after Mg^{2+} starvation, we performed similar analyses. Loss of MgtA and MgtB completely
136 suppressed the loss of viability conferred by the deletion of *corC* or of both *mgpA* and *corC* in stationary
137 phase (Fig. 3A and B), mirroring the effect seen in the Δ*paeA* mutant (7). This similarity implies that the
138 transport of Mg^{2+} via inducible Mg^{2+} transporters serves as a primary factor contributing to the loss of
139 viability in these various mutants, consistent with the concept that Mg^{2+} starvation induces Mg^{2+} uptake
140 leading to excess-cation stress. In contrast, the deletion of polyamine synthesis genes only partially
141 suppressed the phenotypes in the Δ*corC* and the Δ*mgpA* Δ*corC* mutants (Fig. 3C), differing from the
142 complete suppression observed in Δ*paeA* strain (7). These data suggest that while CorC and MgpA have
143 roles in reducing excess-cation stress, these roles are distinct from that of PaeA, which is responsible for
144 reducing cellular polyamine levels.

145 **CorA is not required for CorC to function** The *corC* gene was first identified through a screen
146 for mutations conferring resistance to cobalt (15). In addition to *corC*, this screen identified *corB* and *corA*,
147 the latter encoding the primary Mg^{2+} transporter in Mg-replete conditions, capable of both Mg^{2+} import
148 and efflux (24). Gibson et al. (15) showed that a *corBCD* triple mutant, similar to the *corA* mutant, lost all
149 apparent Mg^{2+} efflux activity. To test if CorA is involved in the *corC* phenotype conferred in stationary
150 phase after Mg^{2+} starvation, we examined the effect of deleting *corA* in the wild-type, Δ*corC*, Δ*mgpA*, and
151 Δ*mgpA* Δ*corC* backgrounds. As shown in figure 3D, the loss of CorA had no significant effect on the

152 Δ*corC* and Δ*mgpA* Δ*corC* phenotypes in stationary phase after Mg^{2+} starvation. Note that CorA does not
153 function at low Mg^{2+} concentrations (25). Indeed, deletion of *corA*, *corB*, and *corD* had no effect on the
154 *corC mgpA* phenotype (Fig. S4).

155 **Loss of CorC confers cobalt and manganese tolerance independent of MgpA.** We also
156 examined the role of CorC and MgpA in Co^{2+} and Mn^{2+} tolerance. As shown in figures 4A-C, deletion of
157 *corC* increased tolerance to both Co^{2+} and Mn^{2+}, similar to the phenotype conferred by deletion of *corA*,
158 consistent with previous data (15). The double deletion of both *corC* and *corA*, which had not been
159 examined in the previous study (15), exhibited a tendency to further increase tolerance to Co^{2+} or Mn^{2+}
160 compared to the single deletion mutants. However, the degree of increase suggests that CorC and CorA
161 act additively and independently. These results indicate that CorC does not require CorA to function.
162 Interestingly, loss of MgpA had little effect on Co^{2+} or Mn^{2+} resistance in an otherwise wild type or *corC*
163 background, but did enhance resistance in a *corA* background (Fig. 4A-C). Importantly, the Δ*paeA*,
164 Δ*mgtA* Δ*mgtB*, Δsynth, and Δsynth Δ*mgtA* Δ*mgtB* mutants showed similar tolerance to Mn^{2+} as the wild
165 type, further showing that the role(s) of CorC and MgpA is distinct from that of PaeA (Fig. 4D and E).

166 ***ΔmgpA and ΔcorC mutants show higher tolerance to exogenous polyamines.*** The data
167 above suggest that the CorC domain-containing proteins, CorC and MgpA, play a role in alleviating
168 excess-cation stress after Mg^{2+} starvation, similar to the general role of PaeA. The specific role of PaeA
169 is to efflux the divalent polyamines, cadaverine and putrescine, the synthesis of which is induced upon
170 Mg^{2+} starvation (8, 14). Indeed, a *paeA* mutant is sensitive to exogenously added putrescine or
171 cadaverine in stationary phase (14). To further examine the effect of the *corC* and *mgpA* genes on excess-
172 cation stress, we measured tolerance to exogenous polyamines after growth in medium with high or low
173 Mg^{2+}. We tested their phenotype in a Δ*paeA* background because this strain is sensitive to polyamines
174 and any additional effects should be easily detectable in this background. Strains were grown in medium
175 with 50 μM $MgCl_2$ (low Mg^{2+}) or 10 mM $MgCl_2$ (high Mg^{2+}), washed, and incubated in a pH 8.5 buffer with
176 the indicated polyamines. This level of low Mg^{2+} does not induce lethality in stationary phase. Note that
177 high pH allows polyamines to be deprotonated and diffuse passively into the cell cytoplasm (14, 26).

178 As expected, the *paeA* mutant, grown to stationary phase in 10 mM Mg^{2+}, is sensitive to either
179 putrescine or cadaverine (Fig. 5). When cells were grown in low Mg^{2+}, the sensitivity to polyamines was
180 significantly reduced, as we have previously shown; it is the combined amount of Mg^{2+} and polyamine
181 that is lethal (7). Deletion of both *corC* and *mgpA* did not further sensitize the *paeA* mutant to
182 polyamines under the conditions we tested, but rather suppressed sensitivity. Deletion of either *corC* or

183 *mgpA* alone had no effect when cells were grown in high Mg^{2+}, but did suppress somewhat when cells
184 were grown in low Mg^{2+} (Fig. 5). These results are consistent with the conclusion that, unlike PaeA,
185 CorC and MgpA are not directly involved in reducing cytoplasmic polyamine levels.

186 ***MgpA and CorC are required for acute systemic infection and for egg white tolerance.***
187 We previously demonstrated that the polyamine efflux transporter PaeA is required for full virulence in
188 mice (7). Interestingly, the virulence attenuation of *paeA* mutant varied depending on the mouse strain:
189 C3H mice, with functional NRAMP1 (SLC11A1), versus BALB/c mice, which have a mutated NRAMP1
190 (27). NRAMP1 is a divalent cation transporter in the phagosomal membrane (28) that restricts
191 *Salmonella* by reducing Mg^{2+} availability in phagosomes (29). The Δ*paeA* strain showed reduced
192 virulence in both strains of mice, but the effect was stronger in the C3H background, supposedly due to
193 lower Mg^{2+} levels in the phagosomes (7). To examine the effect of deleting the *mgpA* and *corC* genes in
194 acute systemic infection *in vivo*, we performed competition assays after intraperitoneal infection (IP) in
195 C3H mice or BALB/c mice. As shown in Table 1, the Δ*corC* Δ*mgpA* strain showed attenuated virulence
196 only in BALB/c mice. In C3H mice, the Δ*mgpA* Δ*corC* strain was equally virulent to the wild type. Note
197 that in the repeat of these experiments (second set of five mice each), the C3H and BALB/c mice were
198 injected with the same inoculum. These results suggest that MgpA and CorC are important for virulence
199 when the Mg^{2+} levels in the phagosome are only moderately limited.

200 To further investigate the role of CorC and MgpA in *Salmonella* pathogenesis, we next focused
201 on egg white tolerance. It was reported that loss of MgpA (YoaE) confers sensitivity to egg white in *S*.
202 Enteritidis, the major serovar linked to human salmonellosis from contaminated eggs (30). We tested
203 egg white tolerance in wild type, Δ*mgpA*, Δ*corC*, and Δ*mgpA* Δ*corC* strains of *S*. Typhimurium. As shown
204 in Figure 6A, deletion of both *mgpA* and *corC* conferred increased sensitivity to egg white, whereas the
205 individual deletions had no effect. The introduction of plasmids encoding either CorC or MgpA suppressed
206 this egg white sensitivity (Fig. 6B). These phenotypes differ from those seen in *S*. Enteritidis, in which
207 the single deletion of the *mgpA* gene resulted in sensitivity to egg white (30). These results indicate that
208 *Salmonella* Typhimurium requires either MgpA or CorC to protect from egg white.

209 To understand the relationship between excess-cation stress and egg white stress, we examined
210 whether other genes involved in reducing excess-cation stress are involved in egg white tolerance. As
211 shown in Figure 6C, mutants lacking PaeA, responsible for polyamine efflux, or MgtA and MgtB, the
212 inducible Mg^{2+} transporters, showed similar viability as the wild type upon egg white exposure, suggesting
213 that these transporters are not involved in egg white tolerance. Interestingly, the Δsynth mutant, lacking

214 genes for polyamine synthesis (7, 14), exhibited sensitivity to egg white, although the degree of viability
215 loss in the Δsynth mutant was smaller than in the Δ*mgpA* Δ*corC* strain (Fig. 6C). These results suggest
216 that polyamine synthesis is required for survival in egg white while polyamine efflux is not necessary.
217 Altogether, we found that MgpA and CorC are required for egg white tolerance and for acute infection in
218 the BALB/c mouse model. Conversely, PaeA is preferentially required for acute infection in the C3H
219 mouse model, and has no apparent role during egg white tolerance. These findings show that the
220 functions of MgpA and CorC are distinct from that of PaeA during *Salmonella* pathogenesis.

221 **MgpA and CorC phenotypes are affected by pH.** Macrophages limit the growth of
222 *Salmonella* not only by restricting Mg^{2+} availability (28, 29), but also by acidifying the phagocytic vacuole
223 (31, 32). In contrast, egg whites are alkaline, with a pH that ranges from 7.6 when fresh to 9.2 as they
224 age (33). The egg whites we used had a pH of about 8.6. This suggests that the phenotypes of the Δ*mgpA*
225 Δ*corC* strains could be influenced by pH. We had tested the impact of deleting either or both the *mgpA*
226 and *corC* genes on survival during stationary phase after Mg^{2+} starvation only at a pH of 7.4 (Fig. 2). To
227 gain insight into the effect of pH on the phenotypes of the Δ*corC* and Δ*mgpA* Δ*corC* strains, we monitored
228 the viability of wild-type, Δ*corC*, Δ*mgpA*, and Δ*mgpA* Δ*corC* strains after Mg^{2+} starvation when grown in
229 acidic (pH 5.5) or alkaline (pH 8.5) N-medium. As shown in figure 7, when grown in acidic medium, the
230 Δ*corC* strain survived after Mg^{2+} starvation for 48 hours at the same level as the wild-type. While the
231 Δ*mgpA* Δ*corC* strain still exhibited a loss of viability in stationary phase when grown without Mg^{2+}, the
232 loss of viability was much reduced compared to that observed in neutral pH medium (Figs. 2C and 7A).
233 In contrast, when grown in alkaline medium, both the Δ*corC* and Δ*mgpA* Δ*corC* strains exhibited a greater
234 loss of viability in stationary phase after Mg^{2+} starvation compared to when grown in neutral pH medium
235 (Figs. 2C and 7B). Altogether, the function of MgpA and CorC becomes more critical for survival in
236 stationary phase after Mg^{2+} starvation as the pH rises.

237 **MgpA and CorC are required for growth and survival in high Mg^{2+} at alkaline pH.** The
238 data above show that MgpA and CorC are essential for survival during the stationary phase after Mg^{2+}
239 starvation, particularly at neutral to alkaline pH. However, the Mg^{2+} concentration in egg white is reported
240 to be 3.7-4.9 mM (34), which typically does not induce Mg^{2+} starvation in *Salmonella in vitro* (13).
241 Therefore, we hypothesized that the Δ*mgpA* Δ*corC* strain is sensitive to Mg^{2+} in egg white at high pH. To
242 test this hypothesis, the wild type, Δ*corC*, Δ*mgpA*, and Δ*mgpA* Δ*corC* strains were pregrown to the mid-
243 exponential phase in pH 7.4 N-minimal medium with 1 mM $MgCl_2$, then washed, diluted into pH 7.4 or
244 pH 8.5 N-minimal medium with increasing amounts of $MgCl_2$, and shaken vigorously at 37°C. OD_{600} and

245 CFU were determined at the indicated time points.

246 When grown in pH 7.4 medium supplemented with 1, 10, or 100 mM $MgCl_2$, all strains exhibited
247 identical growth (Fig. 8A-C) and did not show any loss of viability (Fig. S5A-C). When grown in pH 8.5
248 medium supplemented with 1 mM $MgCl_2$, all strains exhibited identical growth (Fig. 8D) and did not lose
249 viability (Fig. S5D). When grown in alkaline medium supplemented with 10 mM or 100 mM $MgCl_2$, the
250 Δ*mgpA* Δ*corC* strain ceased growth after 3 hours of incubation (Fig. 8E and F) and, at 100 mM Mg^{2+},
251 showed a drastic loss of viability after 12 hours of incubation (Fig. S5F). This phenotype is synthetic; the
252 single deletion mutants showed only minor phenotypes. Collectively, these results show that the Δ*mgpA*
253 Δ*corC* strain is sensitive to high Mg^{2+} in an alkaline medium.

254 We also tested the roles of polyamines and PaeA under these conditions. Importantly, the
255 Δ*paeA* strain did not exhibit any growth defects or loss of viability under high Mg^{2+} stress at pH 7.4 or 8.5
256 (Fig. S6), consistent with CorC and MgpA having functions distinct from that of PaeA. Interestingly, the
257 strain incapable of synthesizing polyamines (Δsynth) showed a severe growth defect at pH 8.5 compared
258 to pH7.4 (Fig S6), but no loss of viability (Fig. S7). This defect was independent of Mg^{2+} concentration.

259 **The *corC* and *mgpA* genes are regulated in response to high Mg^{2+} and pH.** We examined
260 the expression of *corC* and *mgpA* in *Salmonella* using *lacZ* translational fusions. These constructs (Fig.
261 9A), containing the regions upstream of *corC* or *mgpA* and part of the open reading frames fused in frame
262 to *lacZ*, were inserted at the λ *att* site in the chromosome. Thus, the chromosomal *corC* and *mgpA* loci
263 were not disrupted. We measured expression after growth in different pH conditions (acidic [pH 5.5],
264 neutral [pH 7.4], or alkaline [pH 8.5]) and in varying Mg^{2+} concentrations (0, 0.05, or 10 mM $MgCl_2$). Figure
265 9B shows that *corC* expression increased under high Mg^{2+} (10 mM) conditions, regardless of the pH of
266 the medium. Expression of *mgpA* was elevated in high Mg^{2+} (10 mM) when the pH was neutral or alkaline
267 (Fig. 9C). Thus, expression of both CorC and MgpA are induced by high Mg^{2+} concentrations, consistent
268 with their proposed role in combating excess-cation stress, with phenotypes exacerbated at high pH.

269 **Absolute Mg levels are not significantly altered in the *corC* and *mgpA* mutants.** The
270 phenotypes conferred by loss of MgpA and CorC are clearly affected by Mg^{2+} levels in the media. A
271 simple model would suggest that MgpA and CorC either directly or indirectly affect intracellular Mg^{2+}
272 levels. We measured intracellular Mg^{2+} levels using two different methods. Total cellular Mg^{2+} was
273 assayed using inductively coupled plasma mass spectrometry (ICP-MS). Cells were grown to early
274 stationary phase (7.5 hr) as in figure 2. The results indicated that total intracellular Mg^{2+} concentrations
275 were approximately equal in all the various mutants, despite the fact that the *corC mgpA* double mutant

276 had started to lose viability at this time point (Fig. S8).

277 To measure "free" Mg^{2+}, we used a fluorescent Mg^{2+} sensor, MagFET (35). We first confirmed
278 that fluorescence in the MagFRET system was directly proportional to Mg^{2+} concentrations in
279 permeabilized cells (Fig. S9). We are, however, reluctant to draw any conclusions regarding absolute
280 levels of available Mg^{2+} using this system. The wild type, Δ*corC*, Δ*mgpA*, and Δ*mgpA* Δ*corC* strains
281 were grown in N-minimal medium at pH 7.4 with various concentrations of Mg^{2+} and samples were taken
282 at 3 hr, 7.5 hr, and 24 hr. The OD_{600} of each sample was determined (Fig. S10) and then adjusted so
283 that approximately equal numbers of cells were used to measure fluorescence. The CFUs present in
284 each adjusted sample were also determined to measure viability of cells (Fig. S10). Interestingly, in
285 growing cells, free Mg^{2+} concentrations apparently decreased as the Mg^{2+} in the medium increased,
286 suggesting clear regulation of cations in response to the environment (Fig. 10). While total Mg^{2+}
287 concentrations were unchanged in the Δ*mgpA* Δ*corC* double mutant, free Mg^{2+} concentrations were
288 significantly lower at higher external concentrations at both 7.5 hr and 24 hr. Although counterintuitive,
289 loss of CorC and MgpA are clearly affecting cation concentrations or cation distribution in the cell in
290 response to external Mg^{2+} concentrations.

291

292 **DISCUSSION**

293 Maintaining proper cation homeostasis in response to changes in the environment is essential
294 for all living organisms. Previous studies reveal that, upon Mg^{2+} starvation, *Salmonella* induces the Mg^{2+}
295 transporters MgtA and MgtB (9-13) and stimulates the synthesis of polyamines: cadaverine, putrescine,
296 and spermidine (7, 8). Although the specific roles of polyamines are not fully understood, we propose that
297 they act as simple cations that can substitute for Mg^{2+} to neutralize negative charges within cells. Once
298 the Mg^{2+} concentration is re-established, the inner membrane transporter PaeA is required to efflux
299 putrescine and cadaverine from the cell. Otherwise, when *Salmonella* enters stationary phase, the cell
300 experiences what we term "excess-cation stress" (7). In the Δ*paeA* strain, polyamine accumulation occurs,
301 leading to a loss of viability after Mg^{2+} starvation in stationary phase. This loss of viability can be
302 suppressed by deleting the polyamine synthesis genes or the inducible Mg^{2+} transporter genes, showing
303 that it is the combined concentration of polyamines and Mg that is lethal in stationary phase (7).

304 PaeA contains a CorC domain at its C-terminus. Although some CorC domain-containing
305 proteins have been implicated in metal ion homeostasis, the exact function of this domain is not
306 understood. Here we have shown that two additional CorC domain-containing proteins in *Salmonella*,

307 CorC and MgpA (YoaE), play a role in protecting against excess-cation stress in stationary phase. After
308 growth in Mg^{2+}-limiting medium, a *corC* deletion mutant loses viability in stationary phase. Deletion of
309 *mgpA* alone has no effect but confers a synthetic phenotype in the *corC* background; the double mutant
310 suffers a precipitous loss of viability in stationary phase after Mg^{2+} starvation. These proteins act
311 independently of PaeA. Deletion of *paeA* has an apparent additive effect in the *corC* and *corC mgpA*
312 backgrounds, and deletion of *mgpA* confers no additional phenotype in the *paeA* mutant. Loss of
313 viability in the *corC mgpA* double mutant is completely suppressed by loss of the inducible Mg^{2+}
314 transporters, MgtA and MgtB, and partially suppressed by deletion of the polyamine synthesis genes.
315 Thus, CorC and MgpA carry out some seemingly redundant function that is distinct from PaeA, yet all act
316 to prevent excess-cation stress in stationary phase.

317 The concentrations of both Mg^{2+} and polyamines in *Salmonella* range from 5 - 40 mM and are
318 inversely and coordinately regulated by unknown mechanisms (7). Both Mg^{2+} and polyamines have
319 high affinities for phosphate-containing compounds and should compete for binding. For example,
320 putrescine has an ~10-fold higher affinity for ATP than does Mg^{2+} (36). It is also known that putrescine
321 can functionally replace ~80% of the Mg^{2+} in the ribosome (37). The cause of lethality under our
322 conditions is not clear. Simplistically, lethality occurs when the combined concentrations of Mg^{2+} and
323 polyamines are too high. However, it seems more likely that it is competition for binding to some specific
324 compound in the cell that is interfering with an essential function(s). Thus, it is the balance of cations
325 and binding sites that is critical, rather than absolute levels. Our data are all consistent with PaeA
326 exporting putrescine and cadaverine (7, 14). Previous data implicate CorC in Mg^{2+} efflux (15). Given
327 the apparent redundancy between MgpA and CorC, as evidenced by the synthetic phenotypes, we
328 presume that MgpA is also an ion transporter. However, given our overall results, we cannot conclude
329 that CorC or MgpA are directly involved in Mg^{2+} transport. Rather, they could control some other ion
330 that is competing with, or for, Mg^{2+} and polyamines.

331 Further evidence shows that CorC/MgpA are functionally distinct from PaeA. The Δ*paeA*
332 mutant, grown to stationary phase and suspended in high pH buffer, is sensitive to added cadaverine or
333 putrescine (14). The polyamines are deprotonated at high pH, passively enter the cells, and, in the
334 absence of PaeA, build to lethal concentrations. This lethality can be moderated by pre-growing the cells
335 in low Mg^{2+} (7). Loss of CorC and MgpA partially suppresses this sensitivity to polyamines. In this
336 situation, where polyamines continue to enter the cytoplasm, the functions of CorC and MgpA negatively
337 affect survival. One possibility is that the increased levels of polyamines compete with Mg^{2+}, and this

338 liberated Mg^{2+} results in a shift in ion balance and loss of viability. In trying to compensate for this stress,
339 CorC and MgpA are contributing to cation imbalance in this unusual situation.

340 Loss of CorC confers resistance to a high concentration of Mn^{2+} or Co^{2+} in the medium. MgpA
341 has a more minor role in this phenotype. Loss of CorA also confers resistance to Mn^{2+} or Co^{2+}, as
342 previously shown (15). Deletion of *corC* in the *corA* background confers additional protection. CorA also
343 did not affect lethality in stationary phase after Mg^{2+} starvation. Thus, CorC acts independently of CorA.
344 Indeed, none of the previous cobalt-resistance loci, *corA*, *corB*, or *corD* (15), affect lethality in stationary
345 phase after Mg^{2+} starvation. When extracellular Mn^{2+} or Co^{2+} enter the cytoplasm, the functions of CorC
346 and MgpA negatively impact cell survival. These results suggest that, analogous to sensitivity to
347 external polyamines, when Mn^{2+} or Co^{2+} enter the cytoplasm, primarily through CorA-dependent
348 mechanisms (38, 39), the increased levels of Mn^{2+} or Co^{2+} compete with and liberate Mg^{2+}. CorC and
349 MgpA are somehow adjusting ion concentrations to compensate, but this results in increased toxicity and
350 a loss of viability (Fig. 4A-C).

351 The Δ*corC* Δ*mgpA* mutant also behaves very differently than the Δ*paeA* mutant in two virulence
352 models. The Δ*corC* Δ*mgpA* double mutant is sensitive to egg white, whereas loss of PaeA has no
353 apparent effect. Huang et al. (30) demonstrated that the combination of high pH and a small peptide
354 (smaller than 3 kDa) that is sensitive to proteinase K is necessary for egg white to kill the *mgpA* (*yoaE*)
355 strain in *S*. Enteritidis. Further investigation into the molecular mechanisms of MgpA and CorC will deepen
356 our understanding of how egg white kills *Salmonella*.

357 The Δ*corC* Δ*mgpA* mutant is also attenuated in competition assays in BALB/c mice, but, strikingly,
358 there is no phenotype in C3H mice (Table 1). In contrast, the Δ*paeA* mutant shows a stronger
359 attenuation in C3H mice, although there is still some phenotype in the BALB/c background (7).
360 NRAMP1 is a divalent cation transporter in the phagosomal membrane that restricts *Salmonella* by
361 reducing Mg^{2+} availability in phagosomes (28, 29). C3H mice have a functional NRAMP1 (SLC11A1),
362 while BALB/c mice have a mutated NRAMP1 (27). It is clear that the macrophage phagosome in BALB/c
363 is low in Mg^{2+} because the PhoPQ operon is strongly induced (7, 40). Presumably, the Mg^{2+}
364 concentration is higher in the BALB/c phagosome than in the C3H phagosome, which could explain the
365 increased sensitivity of the Δ*corC* Δ*mgpA* mutant. However, we cannot rule out other parameters in the
366 phagosome that could differ between the mouse strains, affecting the overall environment and/or
367 *Salmonella*'s regulatory response.

368 The pH of the media affects the phenotypes. The *corC mgpA* mutant loses viability after growth

369 in Mg^{2+} starvation conditions in pH 7.4 or 8.5 medium. However, this phenotype is dramatically reduced
370 when the pH of the medium is 5.5. High pH also enhances sensitivity to high Mg^{2+} in the medium; the
371 *corC mgpA* mutant cannot grow in pH 8.5 medium when the Mg^{2+} concentration is ≥ 10 mM, whereas the
372 mutant grows fine in pH 7.5 medium, even at 100 mM Mg^{2+}. There are several possibilities for these
373 phenotypic differences at acidic, neutral, and alkaline pH. One possibility is that there are one or more
374 redundant systems that reduce excess-cation stress in acidic environments. For example, PaeA and
375 the cadaverine exporter CadB are redundant in acidic conditions (7). Another possibility is that the
376 stress itself is reduced or alleviated in acidic environments, such that CorC and MgpA are no longer
377 required. High pH in the medium can also significantly affect the activity of bacterial transporters,
378 particularly those that rely on proton-motive force (41). Thus, under high pH conditions, bacteria might
379 be particularly sensitive to high or low cation concentrations in the medium. However, these phenotypes
380 are seemingly contradictory to the mouse phenotypes, given that the macrophage phagosome is low pH.
381 Further investigation is necessary to address these questions.
382 Consistent with their roles in protecting against excess-cation stress, we demonstrated that
383 *mgpA* expression is elevated in high Mg^{2+} (10 mM) when the pH is neutral or alkaline (Fig. 9C), whereas
384 *corC* expression increases under high Mg^{2+} (10 mM) conditions, regardless of the pH of medium (Fig.
385 9B). These results support the model that CorC and MgpA are involved in mitigating excess-cation
386 stress, specifically high Mg^{2+} stress. The regulatory mechanisms governing *mgpA* and *corC* expression
387 remain unclear. Chadani et al. showed that the translation of the N-terminal region of CorC (YbeX)
388 contains an intrinsic ribosome destabilization (IRD) sequence (42). This IRD sequence destabilizes the
389 translating ribosomal complex, leading to premature termination of translation under conditions in which
390 ribosome function is reduced. Low Mg^{2+} stress is a well-known example of ribosome-destabilizing
391 conditions. For example, under such stress, the translation of MgtL, a leader peptide for the inducible
392 magnesium transporter MgtA, stalls due to an IRD mechanism, resulting in the upregulation of *mgtA*
393 expression (43, 44). Consequently, CorC expression is likely upregulated when cytoplasmic Mg^{2+} levels
394 exceed a certain threshold. As for *mgpA* regulation, a leader peptide, YoaL, overlaps with the upstream
395 region of the *mgpA* gene (Fig. 9A; (45). Replacing the start codon of YoaL with a stop codon leads to
396 decreased MgpA translation (46). This suggests that YoaL might play a role in upregulating *mgpA*
397 expression in response to high Mg^{2+} levels. Further research is required to test this hypothesis and to
398 identify the signals that influence this leader peptide-mediated regulation of *mgpA* expression.
399

400 Based on the presence of a transmembrane TerC-domain in the N-terminus of MgpA (**Fig. 1**),
401 which is similar to a protein in *Bacillus subtilis* known to be involved in Mn transport (47), MgpA appears
402 to function directly as a cation transporter. In contrast, CorC, unlike other CorC domain-containing
403 proteins, is cytoplasmic and contains only a CBS-pair domain and the CorC domain (**Fig. 1**). Studies
404 have shown that inactivation of the *corC* gene results in decreased Mg^{2+} efflux activity under high Mg^{2+}
405 conditions. When *corC* is inactivated along with *corB* and *corD* (*apaG*) genes, Mg^{2+} efflux activity is
406 completely lost (15). These data would suggest that CorC regulates a protein responsible for Mg^{2+} efflux
407 activity, although we cannot rule out regulation of some other ion that is competing for Mg^{2+}. However,
408 the protein that CorC regulates does not appear to be CorA, CorB, CorD, or any other CorC-domain-
409 containing proteins, including MgpA, because deletion of the *corC* gene in strains lacking these proteins
410 still confers phenotypes. Therefore, we hypothesize that CorC mitigates excess-cation stress, in
411 response to Mg^{2+} levels, by regulating an uncharacterized transporter. This also leads to the general
412 conclusion that the CorC domain, likely in conjunction with the CBS domain, is regulatory, perhaps
413 sensing levels of cytoplasmic cations. Indeed, a crystal structure of the CorB CBS-pair from the
414 thermophilic archaeon *Methanoculleus thermophilus* shows that dimerization is dependent on binding of
415 ATP- Mg^{2+}, with the Mg^{2+} ion coordinated between the dimers (16), potentially providing a mechanism for
416 sensing relative Mg^{2+} levels.

417 Mg^{2+} is critical for ribosome assembly, function, and stability (4, 6). It is also required for stability
418 of the outer membrane, neutralizing the negative charges in outer membrane lipopolysaccharide (LPS)
419 (5, 48). Indeed, low Mg^{2+} induces stress on outer membrane homeostasis and biogenesis (49).
420 Interestingly, the *corC* gene is in an operon downstream of *ybeZ* and *ybeY*, and upstream of *lnt*. In
421 addition to the promoter upstream of *ybeZ*, there is a start site of transcription between *ybeY* and *corC*
422 (Fig 9; (21, 50)). YbeY is an endoribonuclease with pleiotropic effects on ribosome maturation and
423 function (51). The upstream YbeZ is a putative RNA helicase that is also proposed to participate in
424 ribosome maturation (52). Lnt (CutE), encoded downstream of CorC, is an essential protein required
425 for the final acylation of the N-terminal Cys residue of processed outer membrane lipoproteins (53),
426 including the major lipoprotein Lpp, which tethers the outer membrane to the peptidoglycan (54).

427 Sarigul et al. (22) explored the role of CorC in ribosome metabolism in *E. coli*. They
428 demonstrated that a *corC* deletion mutant exhibited an extended lag phase coming out of stationary
429 phase, particularly when cells were grown at elevated temperatures and under low Mg^{2+} conditions. The
430 *corC* mutant also displayed increased sensitivity to several ribosome-targeting antibiotics. The

431 accumulation of 17S pre-rRNA, a precursor of 16S rRNA, and partial degradation intermediates of 16S
432 rRNA were noted in the *corC* deletion strain upon entering stationary phase. Importantly, the growth
433 phenotypes were suppressed by adding additional Mg^{2+} to the growth medium. Orelle et al. (55)
434 constructed an *E. coli* "Ribo-T" strain that expresses an engineered hybrid rRNA composed of both 16S
435 and 23S rRNA such that the ribosome subunits are tethered and inseparable. A strain making only
436 these engineered ribosomes grew slowly. Selecting for a faster growing mutant yielded a nonsense
437 mutation in *corC,* together with a missense mutation in *rpsA*. Thus, loss of CorC affects ribosome
438 stability and/or function in a Mg^{2+} dependent manner. Overall, the coordinate regulation of these various
439 genes suggests that CorC has an important role in both Mg^{2+}-dependent ribosome function and outer
440 membrane stability. Further investigation into the biochemical function of CorC and MgpA is required to
441 understand how these proteins reduce excess-cation stress after Mg^{2+} starvation and how regulation of
442 cation levels affects overall cell physiology and survival in host tissues.
443

444 **EXPERIMENTAL PROCEDURES**

445 **Media.** During construction of strains, bacteria were routinely grown at 37°C in Luria-Bertani (LB) medium
446 containing 1% NaCl. Strains containing temperature-sensitive plasmids pCP20 and pKD46 were grown at
447 30°C. When necessary, antibiotics were used at the following concentrations: ampicillin, 50 µg/ml;
448 chloramphenicol, 10 µg/ml; kanamycin, 50 µg/ml; apramycin, 50 µg/ml. N-minimal medium (9, 56) contains 5
449 mM KCl, 7.5 mM $(NH_4)_2SO_4$, 0.5 mM K_2SO_4, 1 mM KH_2PO_4, 0.1 M Tris, 15 mM glycerol, and 0.1% casamino
450 acid. The pH was adjusted as indicated. MOPS medium (57), adjusted to pH 7.4 with KOH, contains 40 mM
451 MOPS, 4 mM Tricine, 9.5 mM NH_4Cl, 0.276 mM K_2SO_4, 50 mM NaCl, and 0.1 % casamino acids. When
452 indicated, 1.32 mM K_2HPO_4 and 10 mM $MgCl_2$ were added. We did not add the trace metals listed in the
453 original recipe (57) to minimize the effects of metal addition.
454 **Bacterial strains and plasmids.** Strains are described in Table S1, while plasmids are listed in Table S2. All
455 *Salmonella* strains used are derivatives of *Salmonella enterica* serovar Typhimurium strain 14028. Deletions
456 with concomitant insertion of antibiotic resistance cassettes were constructed using λ Red-mediated
457 recombination as previously described (58, 59), with the indicated endpoints (Table S1). Deletions were
458 verified by PCR analysis, and then transduced into the approrpiate backgrounds using phage P22 HT105/1
459 int-201 (60). All plasmids were passaged through a restriction-minus modification-plus Pi^+ *Salmonella* strain
460 (JS198) (59) prior to transformation into *Salmonella* strains. Antibiotic resistance cassettes were removed
461 using the pCP20 plasmid. The resulting deletions were confirmed by PCR.

462 The translational out of locus *corC'-'lacZ* and *mgpA'-'lacZ* translational fusions were constructed by
463 introducing the regulatory regions of *corC* and *mgpA*, along with the first or twentieth amino acids of the ORFs,
464 respectively, amplified by PCR using primers listed in Table S3, upstream and in-frame with the promotorless
465 *lacZ* in the pDX1 vector via Gibson assembly (NEBuilder® HiFi DNA Assembly)(Fig 9). The resulting product
466 was transformed into DH5α λ*pir*, and the plasmid was confirmed by DNA sequencing. The plasmids, pDX1-
467 *corC-lacZ* and pDX1-*mgpA-lacZ*, were integrated into the λ-attachment site in the *Salmonella* chromosome,
468 as previously described (61). The primers used and the endpoints of the cloned fragments are indicated in
469 Tables S3 and S2, respectively.
470 To construct the pS2513-MagFRET plasmid, the ratiometric fluorescent indicator protein PHP in the
471 pS2513-PHP plasmid (62), a derivative of pSEVA2513 with the constitutive P_{EM7} promoter and the oriV
472 (RSF1010) origin, was replaced with MagFRET from pCMVMagFRET-1 (35) via Gibson assembly
473 (NEBuilder® HiFi DNA Assembly). The primers and plasmids used and the endpoints of the cloned fragments
474 are indicated in Tables S3 and S2, respectively.
475 **β-galactosidase assay.** Overnight cultures grown in N-minimal medium (pH 7.4) supplemented with 10 mM
476 $MgCl_2$ were diluted into the same medium and grown for 4 hours. The cells were then washed three times
477 with 0.85% NaCl and diluted to an OD_{600} of 0.025 in 25 mL of N-minimal medium (pH 5.5, pH 7.4, or pH 8.5)
478 with the indicated amount of $MgCl_2$ in a 125 mL baffled flask, followed by incubation at 37°C. After 24 hours,
479 1 mL of culture was harvested, the cells were pelleted, resuspended in Z buffer, and assayed for β-
480 galactosidase activity in a microtiter plate format, as previously described (63). The β-galactosidase activity
481 units are defined as (μmol of ortho-nitrophenol formed per minute) $x10^6$ / (OD_{600} x mL of cell suspension) and
482 are presented as the mean ± standard deviation with n = 6.
483 **Survival assay.** Overnight cultures, grown in N-minimal medium (pH 7.4) supplemented with 10 mM $MgCl_2$,
484 were washed with 0.85% NaCl three times, diluted to an OD_{600} value of 0.0375 into 5 mL of N-minimal medium
485 with the indicated amount of $MgCl_2$, and incubated at 37°C on a roller drum in a 20 x 150 mm tube. Before
486 and after incubation, serial dilutions of the cultures were plated on LB agar plates that were incubated
487 overnight at 37°C to determine CFU. For the growth curves, the OD_{600} of 250 μL of culture was measured in
488 a BioTek ELx808 Absorbance Reader at the indicated time points. When necessary, the cultures were diluted
489 in the original growth medium to accurately measure the OD_{600} value.
490 **Mn^{2+} and Co^{2+} sensitivity assay.** Overnight cultures, grown in modified MOPS medium (pH 7.4)
491 supplemented with 15 mM glycerol, 1.32 mM K_2HPO_4, and 10 mM $MgCl_2$ were washed three times with 0.85%
492 NaCl, diluted to an OD_{600} value of 0.05 into 10 mL of modified MOPS medium (pH 7.4) supplemented with 15

493 mM glycerol and with or without 1 mM $MnCl_2$ or 0.2 mM $CoCl_2$ in 125 mL baffled flask, and incubated at 37°C
494 for 9 hours. Before and after incubation, serial dilutions of the cultures were plated on LB agar plates that were
495 incubated overnight at 37°C to determine CFU.
496 **Polyamine sensitivity assay.** Polyamine stocks were prepared at 500 mM in 0.85% NaCl with HEPES buffer
497 (pH 8.5). Overnight cultures, grown in N-minimal medium (pH 7.4) supplemented with 10 mM $MgCl_2$ were
498 washed three times with 0.85% NaCl, then diluted 1:200 into 5 mL of N-minimal medium containing either 50
499 μM or 10 mM $MgCl_2$. These cultures were incubated at 37°C on a roller drum for 24 hours. Then, cells were
500 washed three times, resuspended in the same volume of 0.85% NaCl with HEPES buffer (pH 8.5), and
501 aliquoted into 1 mL portions in 13 x 100 mm test tubes. The indicated amounts of cadaverine, putrescine, or
502 spermidine were added, and the cultures were incubated at 37°C on a roller drum. At 0 and 24 hours, serial
503 dilutions of the cultures were plated on LB agar plates and incubated overnight at 37°C to determine the CFU.
504 **Egg white sensitivity assay.** Eggs were purchased from the Meat & Egg Sales Room in the Department of
505 Animal Sciences in the University of Illinois at Urbana-Champaign and stored at 4 °C until used (< one month).
506 Egg white was collected from the eggs and mixed with a 4:1 volume of 0.85% NaCl. The mixture was
507 homogenized on ice using a mortar and pestle, and debris was removed by centrifugation. The resulting
508 solution was used as an 80% egg white solution. Note that these egg white solutions did not contain microbes
509 capable of growing on an LB plate. Overnight *Salmonella* cultures grown in N-minimal medium (pH 7.4)
510 supplemented with 10 mM $MgCl_2$ were diluted into the same medium and grown for 4 hours. The cells were
511 then washed three times with 0.85% NaCl and diluted to an OD_{600} of 0.02 in 1mL of 80% egg white solution
512 or 0.85% NaCl in 13 x 100 mm test tubes. The cultures were incubated at 37°C on a roller drum. At 0 and 24
513 hours, serial dilutions of the cultures were plated on LB agar plates that were incubated overnight at 37°C to
514 determine the CFU.
515 **Animal assay.** All of the animal work was reviewed and approved by the University of Illinois IACUC and was
516 performed under the protocol number 21197. The competition experiments were performed using 5 to 6-week-
517 old mice. The BALB/cAnNHsd and C3H/HeNHsd mice were purchased from Envigo. The *Salmonella* strains
518 were grown overnight in LB medium, mixed 1:1, and diluted to a target inoculum of approximately 1,000 CFU
519 in 200 μL sterile PBS. The mice were infected via the intraperitoneal route. Each inoculum was plated on LB
520 medium to measure the total inoculum and was replica plated to the appropriate selective medium in order to
521 calculate the input ratio for each strain. After 4 days of infection for the BALB/cAnNHsd mice or 5 days of
522 infection for the C3H/HeNHsd mice, the animals were sacrificed via CO_2 asphyxiation and cervical dislocation,
523 and their spleens and livers were removed and homogenized. Serial dilutions of the spleen and livers

524 homogenates were plated on LB medium and incubated overnight. The resulting colonies were replica plated
525 to the appropriate selective medium in order to calculate the output ratio for each competition. The competitive
526 index (CI) was calculated as (percent strain A recovered/percent strain B recovered)/(percent strain A
527 inoculated/percent strain B inoculated). The statistical comparisons of individual competitions were done using
528 a Student's t tests.

529 **High pH growth assay.** Overnight cultures grown in N-minimal medium (pH 7.4), supplemented with 15 mM
530 glycerol and 1 mM $MgCl_2$, were diluted 800-fold into the same medium and grown for 4.5 hours. The cells
531 were then washed three times with 0.85% NaCl, diluted to an OD_{600} of 0.005 in 10 mL of N-minimal medium
532 (pH 7.4 or 8.5) containing 15 mM glycerol and 1, 10, or 100 mM $MgCl_2$, and incubated at 37°C in a 125 mL
533 baffled flask. The OD_{600} of culture was measured using a BioTek ELx808 Absorbance Reader at the indicated
534 time points. When necessary, cultures were diluted in the original growth medium to ensure accurate OD_{600}
535 measurements. To determine CFU, serial dilutions of the cultures were plated on LB agar plates and incubated
536 overnight at 37°C.

537 **Mg^{2+} measurements via inductively coupled plasma-mass spectrometry (ICP-MS).** The cells were
538 cultured as described above for the survival assays. After 7.5 h, cells were collected by centrifugation (7,000
539 x *g*) and washed twice with 0.85% NaCl. The cell pellets were dried at room temperature and were sent to the
540 University of Georgia Center for Applied Isotope Studies for the determination of the total Mg content. The
541 concentration is reported as µg per g of dry weight and is converted to an intracellular concentration assuming
542 2.8×10^{-13} g per cell (64) and 2.3×10^{-15} L per cell (65).

543 **Free-Mg^{2+} measurements via MagFRET.** To obtain a calibration curve, wild-type cells harboring pS2513-
544 MagFRET, pre-grown to mid-exponential phase in N-minimal medium (pH 7.4) with 1 mM $MgCl_2$, were washed
545 and suspended to an OD_{600} of 0.1 in N-minimal medium (pH 7.4) containing the indicated amounts of $MgCl_2$,
546 50 mM sodium benzoate, and 50 mM methylamine HCl. The cells were then incubated at 30°C for 10 minutes.
547 The fluorescence ratio ($Citrine_{(420/530)}$/$Cerulean_{(420/477)}$) was determined using a BioTek Synergy H1 Hybrid
548 Multi-Mode Reader.

549 To measure free-Mg^{2+} levels, overnight cultures grown in N-minimal medium (pH 7.4), supplemented
550 with 15 mM glycerol and 1 mM $MgCl_2$, were diluted 750-fold into the same medium and grown for 4.5 hours.
551 The cells were then washed three times with 0.85% NaCl, diluted to an OD_{600} of 0.05 in 12 mL of N-minimal
552 medium (pH 7.4 or 8.5) containing 15 mM glycerol and the indicated amount of $MgCl_2$, and incubated at 37°C
553 in a 125 mL baffled flask. After 3, 7.5, and 24 hours, aliquots (1.5 mL) were collected, and the fluorescence
554 ratio (Citrine/Cerulean) was determined at an adjusted OD_{600} of 0.1 using a BioTek Synergy H1 Hybrid Multi-

Mode Reader. To determine CFU, serial dilutions of the cultures were spotted on LB Km agar plates and incubated overnight at 37°C.

ACKNOWLEDGMENTS

We are grateful to Jim Imlay and Cari Vanderpool for valuable discussions and Yekaterina Golubeva for critically reading the manuscript. This study was supported by NIH grant R01 AI163687 to JMS. YI performed the experiments. YI and JMS designed the research and wrote the paper. Both authors edited and approved the final version of the manuscript.

563 **Table 1. Competition assays with the Δ*mgpA* Δ*corC* mutant.**

Strain A[a]	Strain B[a]	Mouse Strain	No. of Mice	Organ	Median CI[b]	*P* value[c]	Fold change[d]
Δ*mgpA* Δ*corC*	WT	C3H	10	Spleen	0.82	NS	~1
				Liver	1.01	0.03	~1
		BALB/c	10	Spleen	0.18	<0.00005	5.6
				Liver	0.10	<0.00005	10.5

564

565 [a] Strains used were 14028 and JS2694.

566 [b] Bacteria were recovered from the spleen and liver after intraperitoneal (i.p.) competition assays. The
567 competitive index (CI) was calculated as (percent strain A recovered/percent strain B recovered)/(percent
568 strain A inoculated/percent strain B inoculated).

569 [c] Unpaired Student's t tests were used to compare the logarithmically transformed CI values to the inocula.
570 NS, not significant.

571 [d] The fold attenuation is 1/CI, reflecting the level of attenuation of strain A relative to strain B.

572

REFERENCES

1. Misra VK, Draper DE. 1998. On the role of magnesium ions in RNA stability. Biopolymers 48:113-135. https://doi.org/https://doi.org/10.1002/(SICI)1097-0282(1998)48:2<113::AID-BIP3>3.0.CO;2-Y
2. Lee SY, Lim CJ, Droge P, Yan J. 2015. Regulation of Bacterial DNA Packaging in Early Stationary Phase by Competitive DNA Binding of Dps and IHF. Sci Rep 5:18146. https://doi.org/10.1038/srep18146
3. Verma SC, Qian Z, Adhya SL. 2019. Architecture of the Escherichia coli nucleoid. PLoS Genet 15:e1008456. https://doi.org/10.1371/journal.pgen.1008456
4. Pontes MH, Yeom J, Groisman EA. 2016. Reducing Ribosome Biosynthesis Promotes Translation during Low Mg(2+) Stress. Mol Cell 64:480-492. https://doi.org/10.1016/j.molcel.2016.05.008
5. Groisman EA, Kayser J, Soncini FC. 1997. Regulation of polymyxin resistance and adaptation to low-Mg2+ environments. Journal of Bacteriology 179:7040-7045. https://doi.org/doi:10.1128/jb.179.22.7040-7045.1997
6. Weiss RL, Kimes BW, Morris DR. 1973. Cations and ribosome structure. 3. Effects on the 30S and 50S subunits of replacing bound Mg 2+ by inorganic cations. Biochemistry 12:450-6. https://doi.org/10.1021/bi00727a014
7. Iwadate Y, Golubeva YA, Slauch JM. 2023. Cation Homeostasis: Coordinate Regulation of Polyamine and Magnesium Levels in Salmonella. mBio 14:e02698-22. https://doi.org/doi:10.1128/mbio.02698-22
8. Duprey A, Groisman EA. 2020. DNA supercoiling differences in bacteria result from disparate DNA gyrase activation by polyamines. PLoS Genet 16:e1009085. https://doi.org/10.1371/journal.pgen.1009085
9. Véscovi EG, Soncini FC, Groisman EA. 1996. Mg²⁺ as an Extracellular Signal: Environmental Regulation of Salmonella Virulence. Cell 84:165-174. https://doi.org/10.1016/S0092-8674(00)81003-X
10. Bader MW, Sanowar S, Daley ME, Schneider AR, Cho U, Xu W, Klevit RE, Le Moual H, Miller SI. 2005. Recognition of Antimicrobial Peptides by a Bacterial Sensor Kinase. Cell 122:461-472. https://doi.org/10.1016/j.cell.2005.05.030
11. Choi J, Groisman EA. 2016. Acidic pH sensing in the bacterial cytoplasm is required for Salmonella virulence. Molecular Microbiology 101:1024-1038. https://doi.org/https://doi.org/10.1111/mmi.13439
12. Snavely MD, Gravina SA, Cheung TT, Miller CG, Maguire ME. 1991. Magnesium transport in Salmonella typhimurium. Regulation of mgtA and mgtB expression. J Biol Chem 266:824-9.

13. Groisman EA, Duprey A, Choi J. 2021. How the PhoP/PhoQ System Controls Virulence and Mg(2+) Homeostasis: Lessons in Signal Transduction, Pathogenesis, Physiology, and Evolution. Microbiol Mol Biol Rev 85:e0017620. https://doi.org/10.1128/MMBR.00176-20
14. Iwadate Y, Ramezanifard R, Golubeva YA, Fenlon LA, Slauch JM. 2021. PaeA (YtfL) protects from cadaverine and putrescine stress in Salmonella Typhimurium and E. coli. Mol Microbiol doi:10.1111/mmi.14686. https://doi.org/10.1111/mmi.14686
15. Gibson MM, Bagga DA, Miller CG, Maguire ME. 1991. Magnesium transport in Salmonella typhimurium: the influence of new mutations conferring Co2+ resistance on the CorA Mg2+ transport system. Molecular Microbiology 5:2753-2762. https://doi.org/https://doi.org/10.1111/j.1365-2958.1991.tb01984.x
16. Chen YS, Kozlov G, Moeller BE, Rohaim A, Fakih R, Roux B, Burke JE, Gehring K. 2021. Crystal structure of an archaeal CorB magnesium transporter. Nat Commun 12:4028. https://doi.org/10.1038/s41467-021-24282-7
17. Huang Y, Jin F, Funato Y, Xu Z, Zhu W, Wang J, Sun M, Zhao Y, Yu Y, Miki H, Hattori M. 2021. Structural basis for the Mg²⁺ recognition and regulation of the CorC Mg²⁺ transporter. Science Advances 7:eabe6140. https://doi.org/doi:10.1126/sciadv.abe6140
18. Armitano J, Redder P, Guimarães VA, Linder P. 2016. An Essential Factor for High Mg(2+) Tolerance of Staphylococcus aureus. Frontiers in microbiology 7:1888-1888. https://doi.org/10.3389/fmicb.2016.01888
19. Quinn MJ, Resch CT, Sun J, Lind EJ, Dibrov P, Hase CC. 2012. NhaP1 is a K+(Na+)/H+ antiporter required for growth and internal pH homeostasis of Vibrio cholerae at low extracellular pH. Microbiology (Reading) 158:1094-1105. https://doi.org/10.1099/mic.0.056119-0
20. Kroner GM, Wolfe MB, Freddolino PL. 2019. Escherichia coli Lrp Regulates One-Third of the Genome via Direct, Cooperative, and Indirect Routes. J Bacteriol 201. https://doi.org/10.1128/JB.00411-18
21. Nonaka G, Blankschien M, Herman C, Gross CA, Rhodius VA. 2006. Regulon and promoter analysis of the E. coli heat-shock factor, sigma32, reveals a multifaceted cellular response to heat stress. Genes Dev 20:1776-89. https://doi.org/10.1101/gad.1428206
22. Sarigul I, Zukova A, Alparslan E, Remm S, Pihlak M, Kaldalu N, Tenson T, Maivali U. 2024. Involvement of Escherichia coli YbeX/CorC in ribosomal metabolism. Mol Microbiol doi:10.1111/mmi.15248. https://doi.org/10.1111/mmi.15248
23. Chinni SV, Raabe CA, Zakaria R, Randau G, Hoe CH, Zemann A, Brosius J, Tang TH, Rozhdestvensky TS. 2010. Experimental identification and characterization of 97 novel npcRNA candidates in Salmonella enterica serovar Typhi. Nucleic Acids Res 38:5893-908. https://doi.org/10.1093/nar/gkq281

24. Snavely MD, Florer JB, Miller CG, Maguire ME. 1989. Magnesium transport in Salmonella typhimurium: 28Mg2+ transport by the CorA, MgtA, and MgtB systems. Journal of Bacteriology 171:4761-4766. https://doi.org/doi:10.1128/jb.171.9.4761-4766.1989
25. Chamnongpol S, Groisman EA. 2002. Mg2+ homeostasis and avoidance of metal toxicity. Mol Microbiol 44:561-71. https://doi.org/10.1046/j.1365-2958.2002.02917.x
26. Yohannes E, Thurber AE, Wilks JC, Tate DP, Slonczewski JL. 2005. Polyamine stress at high pH in Escherichia coli K-12. BMC Microbiol 5:59. https://doi.org/10.1186/1471-2180-5-59
27. Sellers RS, Clifford CB, Treuting PM, Brayton C. 2012. Immunological variation between inbred laboratory mouse strains: points to consider in phenotyping genetically immunomodified mice. Vet Pathol 49:32-43. https://doi.org/10.1177/0300985811429314
28. Nevo Y, Nelson N. 2006. The NRAMP family of metal-ion transporters. Biochimica et Biophysica Acta (BBA) - Molecular Cell Research 1763:609-620. https://doi.org/https://doi.org/10.1016/j.bbamcr.2006.05.007
29. Cunrath O, Bumann D. 2019. Host resistance factor SLC11A1 restricts Salmonella growth through magnesium deprivation. Science 366:995-999. https://doi.org/10.1126/science.aax7898
30. Huang X, Hu M, Zhou X, Liu Y, Shi C, Shi X. 2020. Role of yoaE Gene Regulated by CpxR in the Survival of Salmonella enterica Serovar Enteritidis in Antibacterial Egg White. mSphere 5. https://doi.org/10.1128/mSphere.00638-19
31. Lukacs GL, Rotstein OD, Grinstein S. 1990. Phagosomal acidification is mediated by a vacuolar-type H(+)-ATPase in murine macrophages. Journal of Biological Chemistry 265:21099-21107. https://doi.org/https://doi.org/10.1016/S0021-9258(17)45332-4
32. Forgac M. 2007. Vacuolar ATPases: rotary proton pumps in physiology and pathophysiology. Nat Rev Mol Cell Biol 8:917-29. https://doi.org/10.1038/nrm2272
33. Stadelman WJ, Cotterill OJ. 1995. Egg Science and Technology, Fourth Edition. Haworth Press, Inc.
34. Legros J, Jan S, Bonnassie S, Gautier M, Croguennec T, Pezennec S, Cochet MF, Nau F, Andrews SC, Baron F. 2021. The Role of Ovotransferrin in Egg-White Antimicrobial Activity: A Review. Foods 10. https://doi.org/10.3390/foods10040823
35. Lindenburg LH, Vinkenborg JL, Oortwijn J, Aper SJ, Merkx M. 2013. MagFRET: the first genetically encoded fluorescent Mg2+ sensor. PLoS One 8:e82009. https://doi.org/10.1371/journal.pone.0082009
36. De Stefano C, Giuffrè O, Sammartano S. 1998. Thermodynamic parameters for the binding of ATP by protonated open-chain polyamines. Journal of the Chemical Society, Faraday Transactions 94:1091-1095. https://doi.org/10.1039/A709230J
37. Weiss RL, Morris DR. 1973. Cations and ribosome structure. I. Effects of the 30S subunit of

substituting polyamines for magnesium ion. Biochemistry 12:435-441. https://doi.org/10.1021/bi00727a012

38. Kehres DG, Maguire ME. 2002. Structure, properties and regulation of magnesium transport proteins. Biometals 15:261-270. https://doi.org/10.1023/A:1016078832697
39. Stetsenko A, Guskov A. 2020. Cation permeability in CorA family of proteins. Scientific Reports 10:840. https://doi.org/10.1038/s41598-020-57869-z
40. Golubeva YA, Slauch JM. 2006. Salmonella enterica serovar Typhimurium periplasmic superoxide dismutase SodCI is a member of the PhoPQ regulon and is induced in macrophages. J Bacteriol 188:7853-61. https://doi.org/10.1128/JB.00706-06
41. Slotboom DJ. 2014. Structural and mechanistic insights into prokaryotic energy-coupling factor transporters. Nat Rev Microbiol 12:79-87. https://doi.org/10.1038/nrmicro3175
42. Chadani Y, Sugata N, Niwa T, Ito Y, Iwasaki S, Taguchi H. 2021. Nascent polypeptide within the exit tunnel stabilizes the ribosome to counteract risky translation. EMBO J 40:e108299. https://doi.org/10.15252/embj.2021108299
43. Chadani Y, Niwa T, Izumi T, Sugata N, Nagao A, Suzuki T, Chiba S, Ito K, Taguchi H. 2017. Intrinsic Ribosome Destabilization Underlies Translation and Provides an Organism with a Strategy of Environmental Sensing. Mol Cell 68:528-539 e5. https://doi.org/10.1016/j.molcel.2017.10.020
44. Gall AR, Datsenko KA, Figueroa-Bossi N, Bossi L, Masuda I, Hou Y-M, Csonka LN. 2016. Mg²⁺ regulates transcription of mgtA in Salmonella Typhimurium via translation of proline codons during synthesis of the MgtL peptide. Proceedings of the National Academy of Sciences 113:15096-15101. https://doi.org/10.1073/pnas.1612268113
45. VanOrsdel CE, Kelly JP, Burke BN, Lein CD, Oufiero CE, Sanchez JF, Wimmers LE, Hearn DJ, Abuikhdair FJ, Barnhart KR, Duley ML, Ernst SEG, Kenerson BA, Serafin AJ, Hemm MR. 2018. Identifying New Small Proteins in Escherichia coli. Proteomics 18:e1700064. https://doi.org/10.1002/pmic.201700064
46. Weaver J, Mohammad F, Buskirk AR, Storz G. 2019. Identifying Small Proteins by Ribosome Profiling with Stalled Initiation Complexes. mBio 10. https://doi.org/10.1128/mBio.02819-18
47. He B, Sachla AJ, Helmann JD. 2023. TerC proteins function during protein secretion to metalate exoenzymes. Nat Commun 14:6186. https://doi.org/10.1038/s41467-023-41896-1
48. Groisman EA, Chan C. 2021. Cellular Adaptations to Cytoplasmic Mg2+ Limitation. Annual Review of Microbiology 75:649-672. https://doi.org/10.1146/annurev-micro-020518-115606
49. Ramezanifard R, Golubeva YA, Palmer AD, Slauch JM. 2023. TamAB is regulated by PhoPQ and functions in outer membrane homeostasis during Salmonella pathogenesis. Journal of Bacteriology 205:e00183-23. https://doi.org/doi:10.1128/jb.00183-23

50. Canals R, Hammarlöf DL, Kröger C, Owen SV, Fong WY, Lacharme-Lora L, Zhu X, Wenner N, Carden SE, Honeycutt J, Monack DM, Kingsley RA, Brownridge P, Chaudhuri RR, Rowe WPM, Predeus AV, Hokamp K, Gordon MA, Hinton JCD. 2019. Adding function to the genome of African Salmonella Typhimurium ST313 strain D23580. PLOS Biology 17:e3000059. https://doi.org/10.1371/journal.pbio.3000059
51. Naganathan A, Keltz R, Lyon H, Culver GM. 2021. Uncovering a delicate balance between endonuclease RNase III and ribosomal protein S15 in E. coli ribosome assembly. Biochimie 191:104-117. https://doi.org/https://doi.org/10.1016/j.biochi.2021.09.003
52. Andrews ESV, Patrick WM. 2022. The hypothesized role of YbeZ in 16S rRNA maturation. Arch Microbiol 204:114. https://doi.org/10.1007/s00203-021-02739-z
53. Grabowicz M. 2019. Lipoproteins and Their Trafficking to the Outer Membrane. EcoSal Plus 8:10.1128/ecosalplus.ESP-0038-2018. https://doi.org/doi:10.1128/ecosalplus.esp-0038-2018
54. Narita S-i, Matsuyama S-i, Tokuda H. 2004. Lipoprotein trafficking in Escherichia coli. Archives of Microbiology 182:1-6. https://doi.org/10.1007/s00203-004-0682-4
55. Orelle C, Carlson ED, Szal T, Florin T, Jewett MC, Mankin AS. 2015. Protein synthesis by ribosomes with tethered subunits. Nature 524:119-24. https://doi.org/10.1038/nature14862
56. Nelson DL, Kennedy EP. 1971. Magnesium transport in Escherichia coli. Inhibition by cobaltous ion. J Biol Chem 246:3042-9.
57. Neidhardt FC, Bloch PL, Smith DF. 1974. Culture Medium for Enterobacteria. Journal of Bacteriology 119:736-747. https://doi.org/doi:10.1128/jb.119.3.736-747.1974
58. Datsenko KA, Wanner BL. 2000. One-step inactivation of chromosomal genes in Escherichia coli K-12 using PCR products. Proceedings of the National Academy of Sciences of the United States of America 97:6640-6645. https://doi.org/10.1073/pnas.120163297
59. Ellermeier CD, Janakiraman A, Slauch JM. 2002. Construction of targeted single copy lac fusions using lambda Red and FLP-mediated site-specific recombination in bacteria. Gene 290:153-161. https://doi.org/10.1016/S0378-1119(02)00551-6
60. Maloy SR, Stewart VJ, Taylor RK. 1996. Genetic Analysis of pathogenic bacteria: a laboratory manual. Cold Spring Harbor Laboratory Press, Plainview, NY.
61. Lin D, Rao CV, Slauch JM. 2008. The Salmonella SPI1 type three secretion system responds to periplasmic disulfide bond status via the flagellar apparatus and the RcsCDB system. J Bacteriol 190:87-97. https://doi.org/10.1128/JB.01323-07
62. Arce-Rodriguez A, Volke DC, Bense S, Haussler S, Nikel PI. 2019. Non-invasive, ratiometric determination of intracellular pH in Pseudomonas species using a novel genetically encoded indicator. Microb Biotechnol 12:799-813. https://doi.org/10.1111/1751-7915.13439
63. Slauch JM, Silhavy TJ. 1991. cis-acting ompF mutations that result in OmpR-dependent constitutive expression. Journal of Bacteriology 173:4039-4048.

https://doi.org/doi:10.1128/jb.173.13.4039-4048.1991

64. Neidhardt FC. 1987. Chemical composition of *Escherichia coli*. pp 3–6 In Neidhardt FC (ed), *Escherichia coli* and *Salmonella*: cellular and molecular biology, 2nd ed ASM Press, Washington, DC.

65. Volkmer B, Heinemann M. 2011. Condition-dependent cell volume and concentration of Escherichia coli to facilitate data conversion for systems biology modeling. PLoS One 6:e23126. https://doi.org/10.1371/journal.pone.0023126

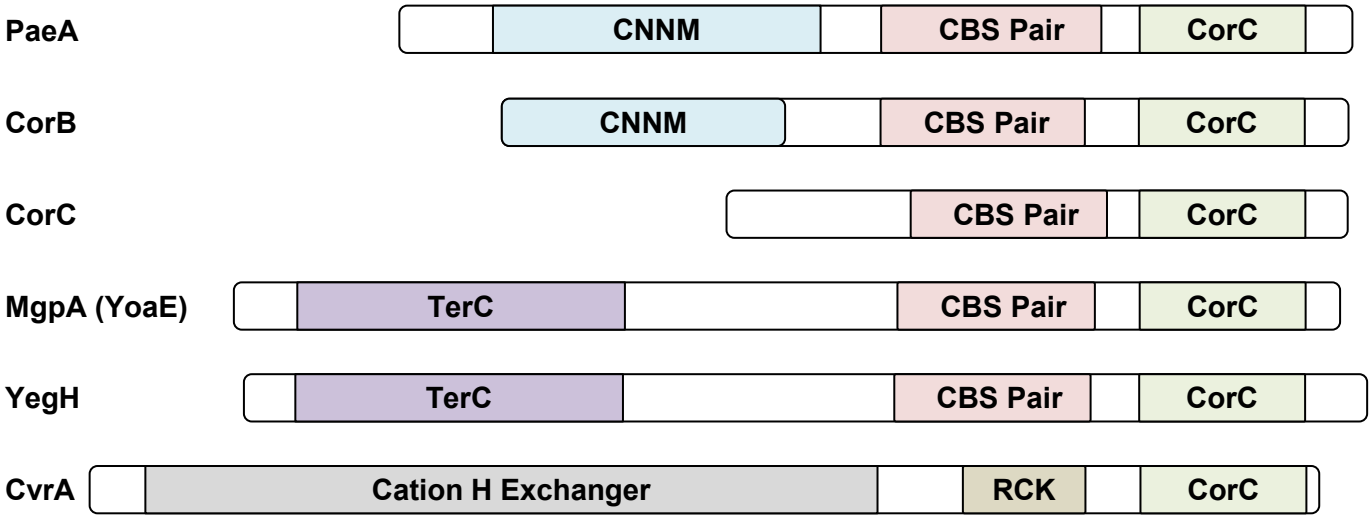

Fig. 1. Domain architecture of CorC domain-containing proteins in *Salmonella*. Conserved domains were predicted using InterPro (https://www.ebi.ac.uk/interpro/). Each domain is represented by a different color, while regions with no domain assignment are shown in white.

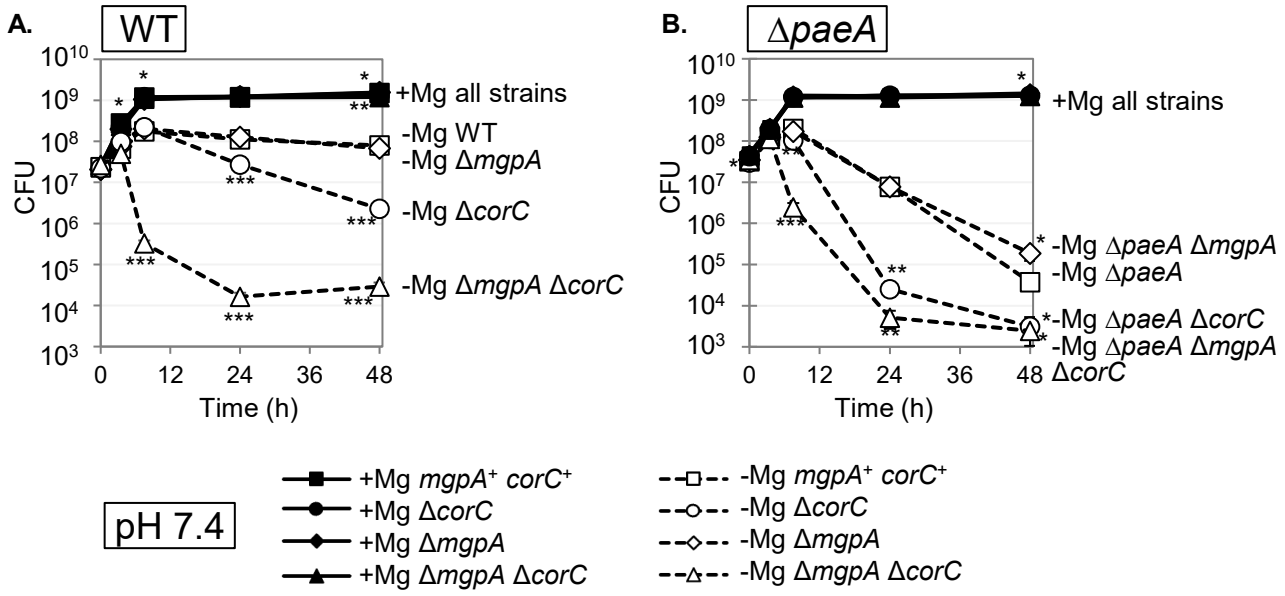

Fig. 2. The Δ*corC* strain loses viability in stationary phase after Mg^{2+} starvation, the deletion of *mgpA* exacerbates the effect. The indicated strains were grown overnight in N-minimal medium pH 7.4 with 10 mM $MgCl_2$, washed, diluted into N-minimal medium pH 7.4 with or without 10 mM $MgCl_2$ (t=0 h), and incubated at 37℃. CFUs were determined at the indicated time points in wild type (A) and ΔpaeA (B) background. Values are mean ± SD, n = 6. Unpaired t test ($p < 0.05$*, 0.005**, 0.0005***) vs *mgpA*$^+$ *corC*$^+$ parent strain at the same time point and at the same Mg^{2+} concentration. Strains used: 14028, JS2692, JS2693, JS2694, JS2695, JS2696, JS2697, and JS2698.

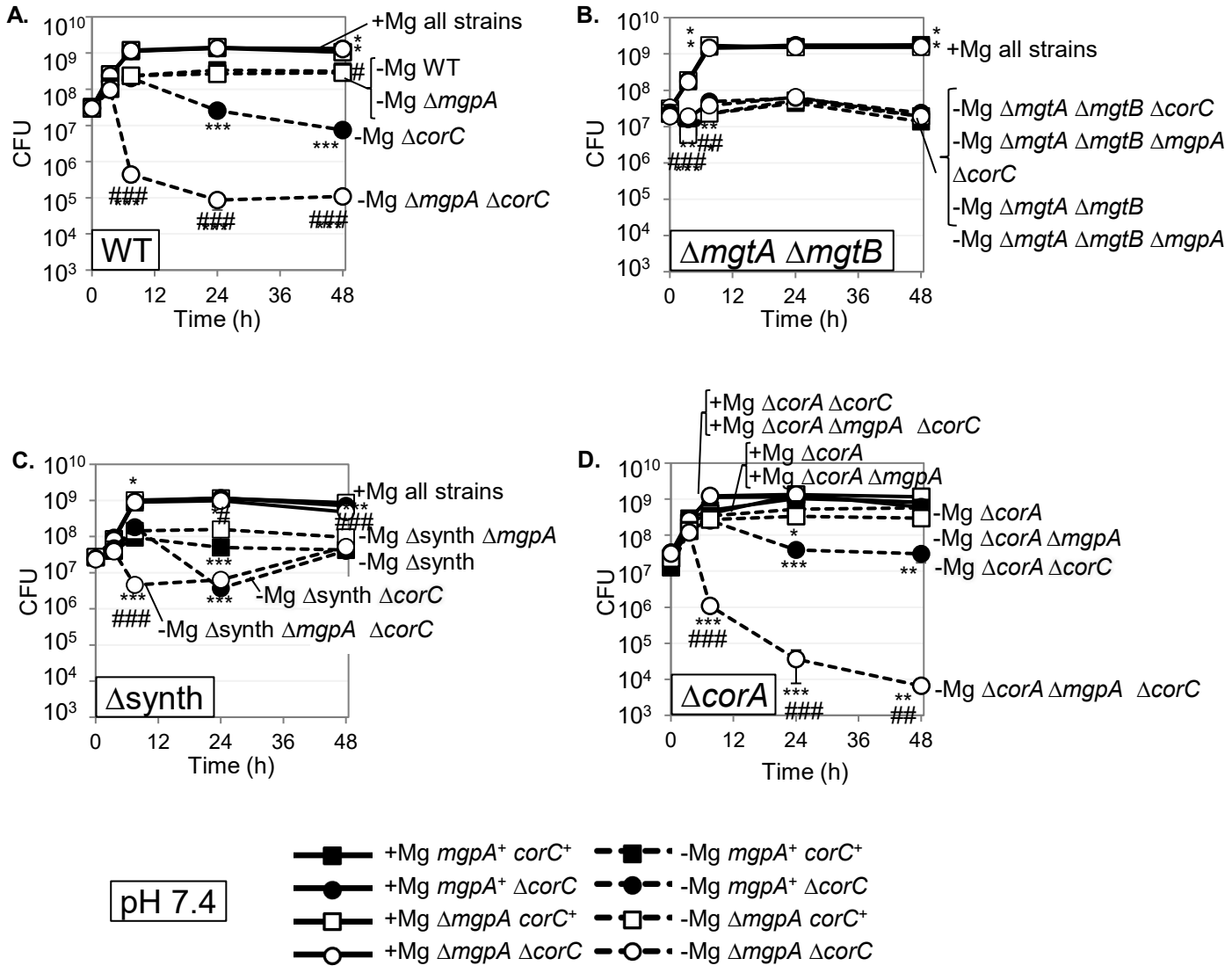

Fig. 3. Loss of the high-affinity Mg^{2+} transporters MgtA and MgtB, but not CorA, suppresses the *corC* phenotype in stationary phase after Mg^{2+} starvation. The indicated strains were grown overnight in N-minimal medium pH 7.4 with 10 mM $MgCl_2$, washed, diluted into N-minimal medium pH 7.4 with or without 10 mM $MgCl_2$ (t=0 h), and incubated at 37℃. CFUs were determined at the indicated time points in WT (A), Δ*mgtA* Δ*mgtB* (B), Δsynth (C), and Δ*corA* (D) background. Values are mean ± SD, n = 6. Unpaired t test ($p < 0.05^{*}$, 0.005^{**}, 0.0005^{***}) versus the *mgpA*+ *corC*+ at the same time point and at the same Mg^{2+} concentration, and ($p < 0.05^{\#}$, $0.005^{\#\#}$, $0.0005^{\#\#\#}$) Δ*mgpA corC*+ versus Δ*mgpA* Δ*corC* at the same time point and at the same Mg^{2+} concentration. Strains used: 14028, JS2692, JS2693, JS2694, JS2713, JS2714, JS2715, JS2716, JS2560, JS2717, JS2718, JS2717, JS2720, JS2721, JS2722, and JS2723.

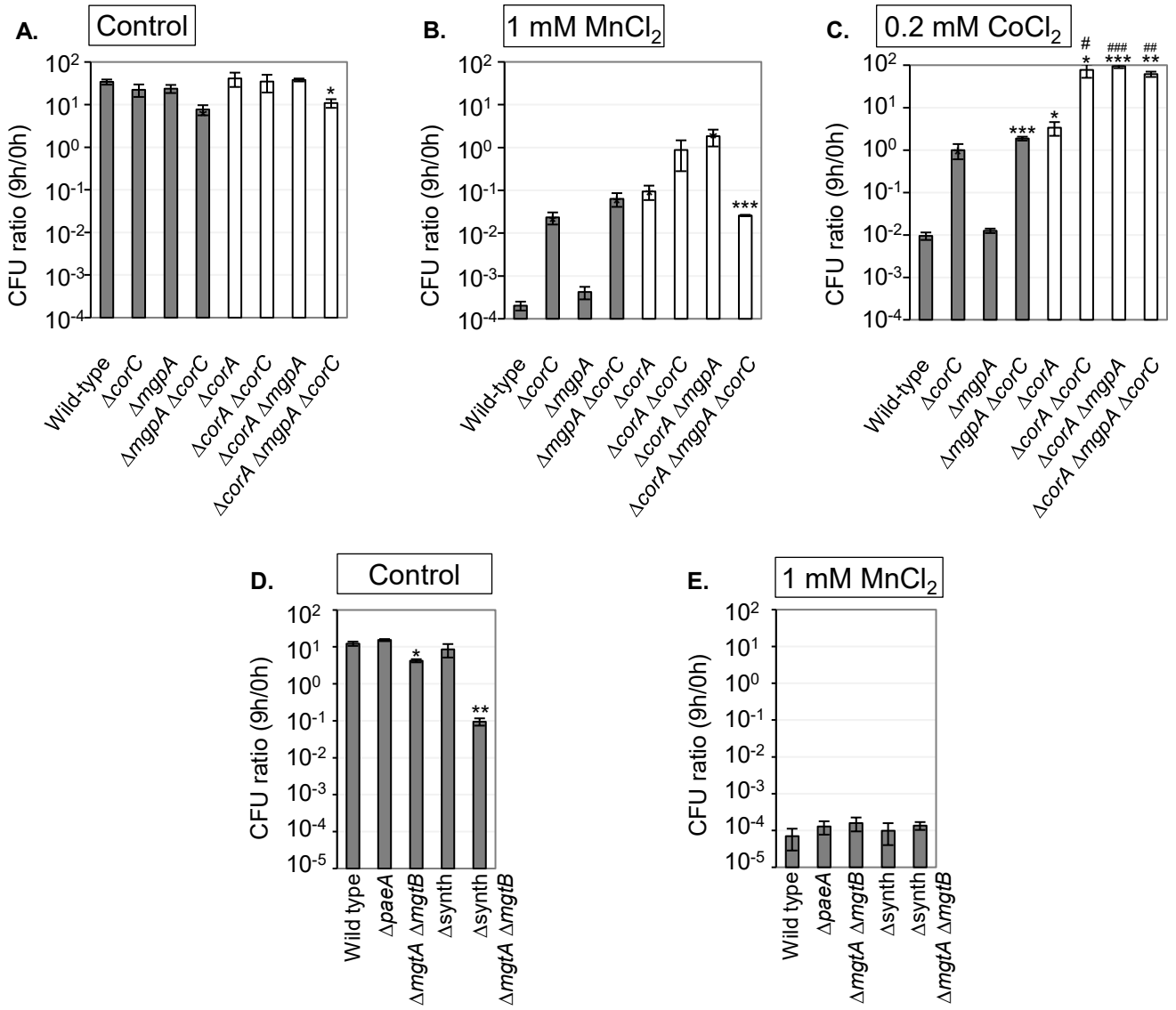

Fig. 4. Loss of CorC, but not MgpA increases tolerance to Co^{2+} and Mn^{2+}. The indicated strains were grown overnight in MOPS-minimal medium (pH 7.4) with 1.32 mM KH_2PO_4 and 10 mM $MgCl_2$, washed, diluted into MOPS-minimal medium (pH 7.4) with or without the indicated amounts of $MgCl_2$ or $CoCl_2$ in the absence of KH_2PO_4 and $MgCl_2$ (t=0h), and incubated at 37℃. CFUs were determined at 0h and 9h. CFU ratio (9h/0h) values are mean ± SD, n = 3. Unpaired t test ($p < 0.05$*, 0.005**, 0.0005***) versus WT and ($p < 0.05^{\#}$, $0.005^{\#\#}$, $0.0005^{\#\#\#}$) versus Δ*corA*. Strains used: 14028, JS2692, JS2693, JS2694, JS2720, JS2721, JS2722, JS2723, JS2430, JS2562, JS2560, and JS2563.

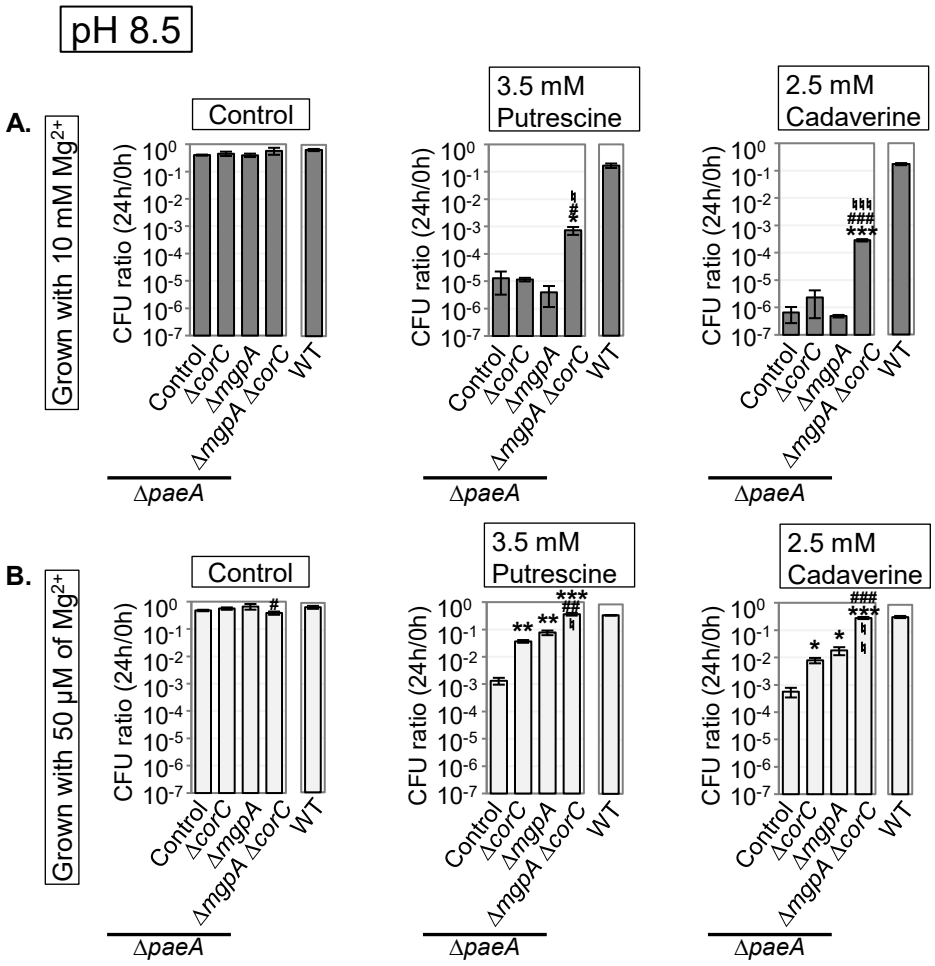

Fig. 5. Loss of CorC and MgpA suppresses polyamine sensitivity in *paeA* background. The indicated strains were grown in N-minimal medium (pH 7.4) with (A) 10 mM or (B) 50 μM $MgCl_2$ for 24 hours at 37℃, washed, diluted into pH 8.5-buffered saline containing indicated polyamines (t=0h), and incubated at 37℃. CFUs were determined at 0h and 24h. CFU ratio (24h/0h) values are mean ± SD, n = 3. Unpaired t test ($p < 0.05^{*}$, 0.005^{**}, 0.0005^{***}) versus WT, ($p < 0.05^{\#}$, $0.005^{\#\#}$, $0.0005^{\#\#\#}$) Δ*mgpA corC*+ versus Δ*mgpA* Δ*corC*, and ($p < 0.05^{\natural}$, $0.005^{\natural\natural}$, $0.0005^{\natural\natural\natural}$) *mgpA*+ Δ*corC* versus Δ*mgpA* Δ*corC*. Strains used: 14028, JS2695, JS2724, JS2725, and JS2726.

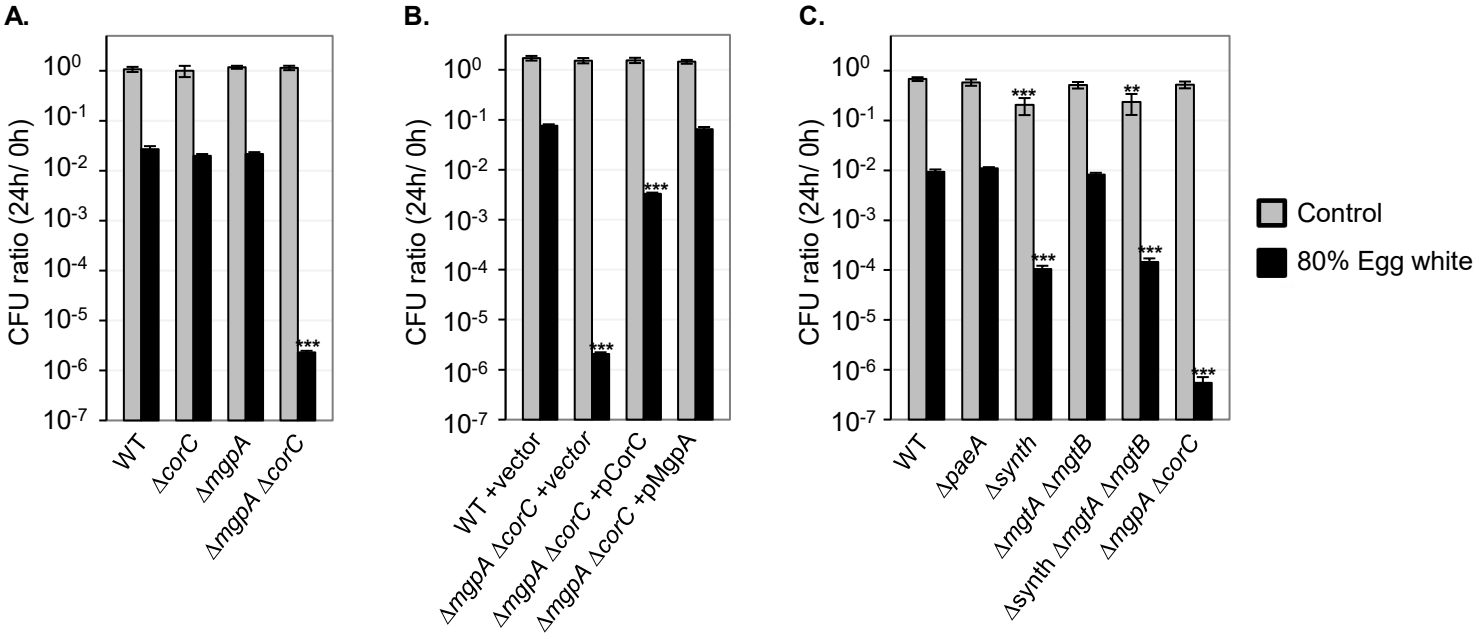

Fig. 6. The Δ*mgpA* Δ*corC* strain is sensitive to egg white. The indicated strains were pre-grown to mid-exponential phase in N-minimal medium (pH 7.4) with 10 mM $MgCl_2$ at 37℃, washed, diluted into 80% egg white solution or PBS (t=0 h), and incubated at 37℃. CFUs were determined at 0h and 24h. CFU ratio (24h/0h) values are mean ± SD, n = 6. Unpaired t test ($p < 0.05$*, 0.005**, 0.0005***) versus WT same treatment. Strains used: 14028, JS2728, JS2729, JS2730, JS2699, JS2731, JS2732, JS2733, JS2430, JS2560, JS2562, JS2563, and JS2694.

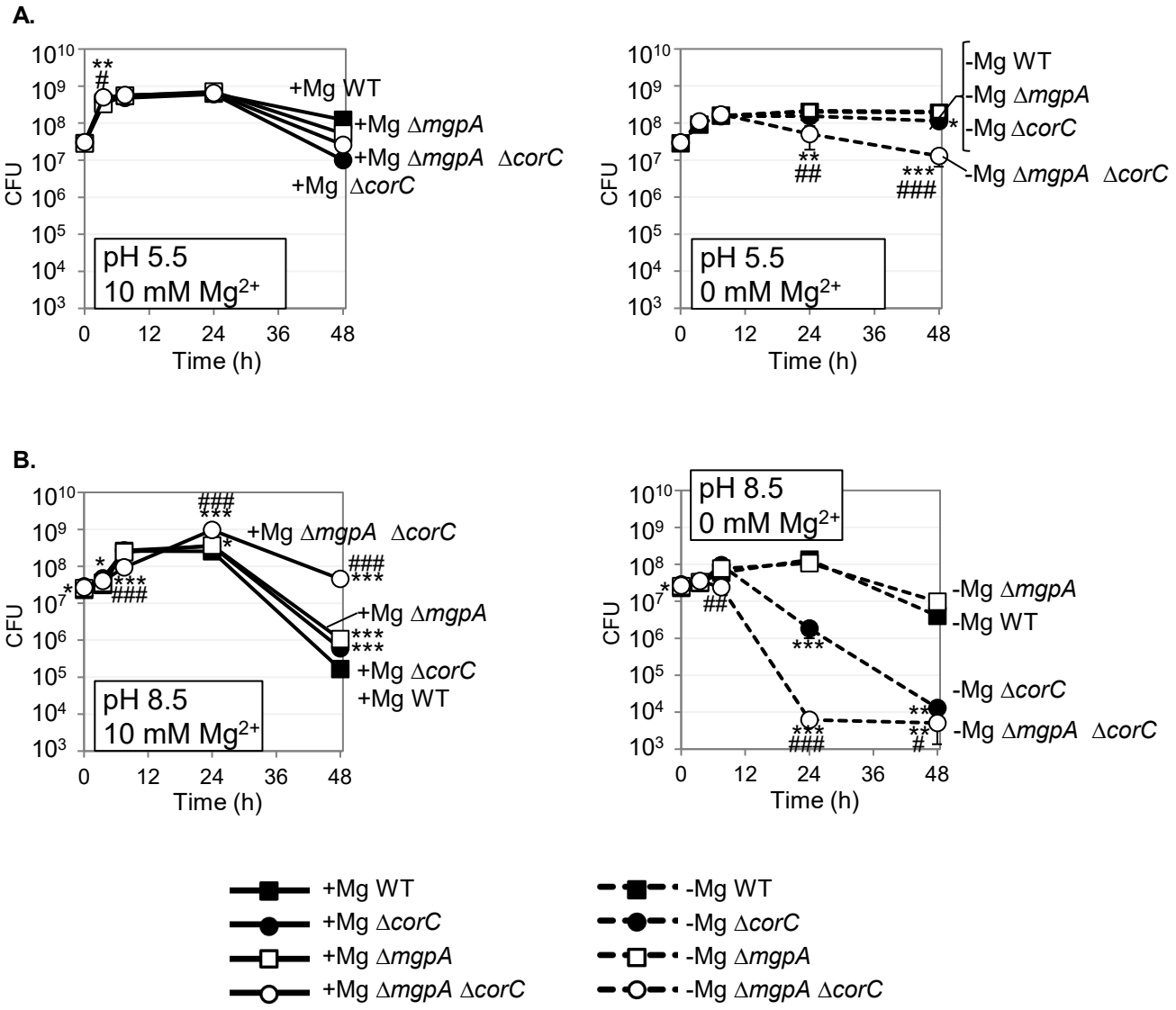

Fig. 7. The loss of viability in Δ*corC* and Δ*mgpA* Δ*corC* strains during stationary phase after Mg^{2+} starvation is reduced in acidic medium and exacerbated in alkaline medium. The indicated strains were grown overnight in N-minimal medium pH 7.4 with 10 mM $MgCl_2$, washed, diluted into N-minimal medium (A) pH 5.5 and (B) pH 8.5 with or without 10 mM $MgCl_2$ (t=0 h), and incubated at 37℃. CFUs were determined at the indicated timepoints. Values are mean ± SD, n = 6. Unpaired t test ($p < 0.05^{*}$, 0.005^{**}, 0.0005^{***}) versus corresponding WT and ($p < 0.05^{\#}$, $0.005^{\#\#}$, $0.0005^{\#\#\#}$) Δ*mgpA corC*+ versus Δ*mgpA* Δ*corC* at the same time point and at the same Mg^{2+} concentration. Strains used: 14028, JS2692, JS2693, and JS2694.

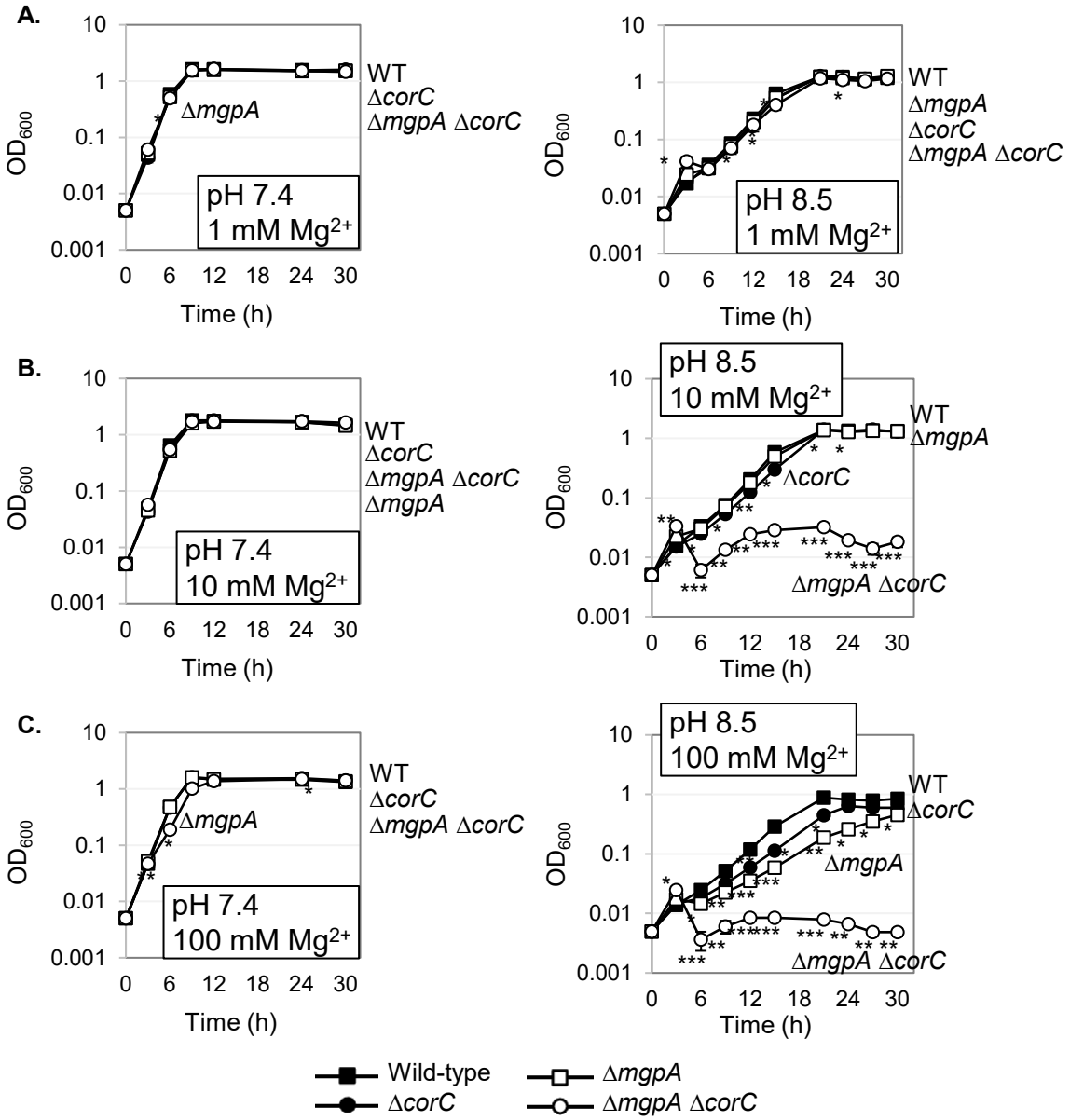

Fig. 8. pH affects growth under high $Mg2^+$ conditions. The indicated strains were pre-grown to mid-exponential phase in N-minimal medium pH 7.4 with 1 mM $MgCl_2$, washed, and diluted into N-minimal medium pH 7.4 or pH 8.5 with (A) 1 mM, (B) 10 mM, and (C) 100 mM $MgCl_2$ (t=0h), and incubated at 37℃. OD_{600} was determined at the indicated timepoints. Values are mean ± SD, n = 3. Unpaired t test ($p < 0.05$*, 0.005**, 0.0005***) versus corresponding WT at the same timepoint. Strains used: 14028, JS2692, JS2693, and JS2694.

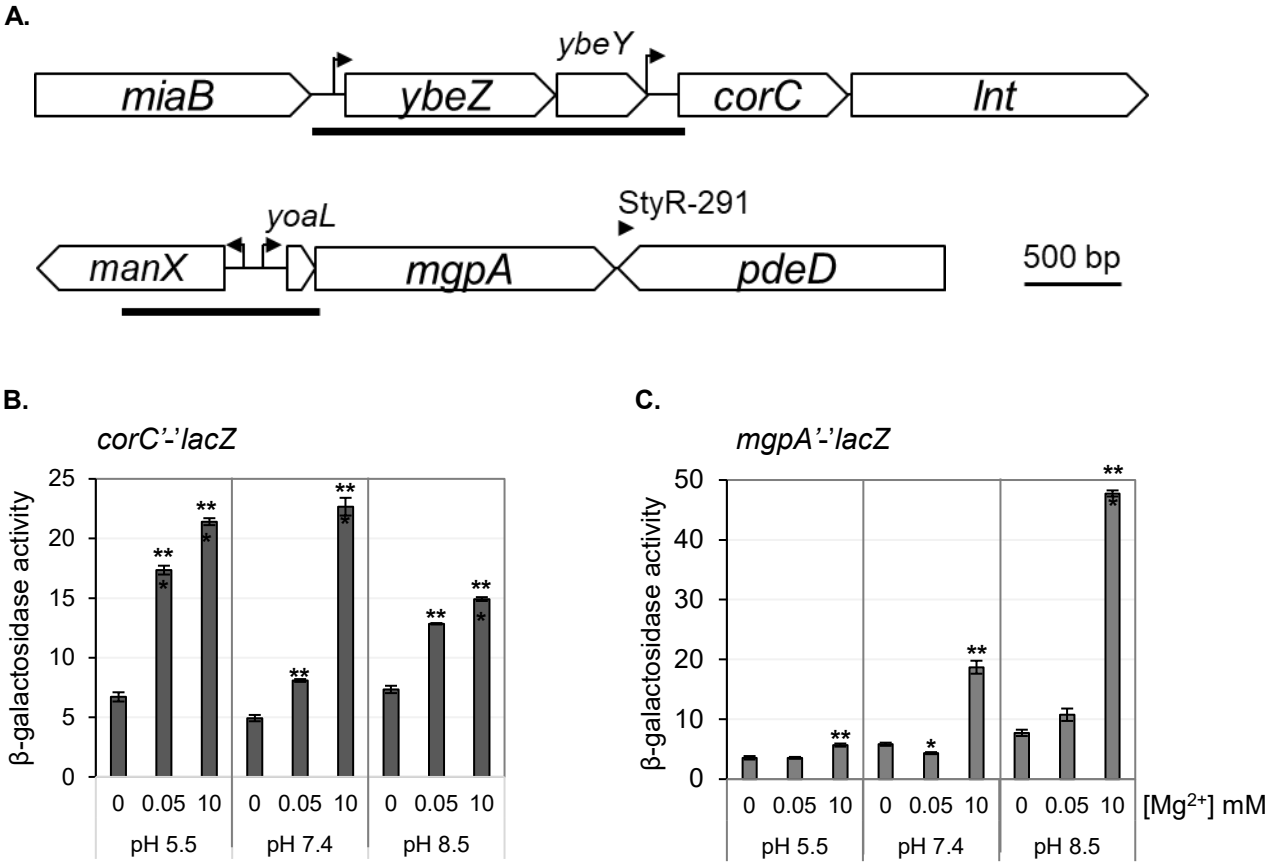

Fig 9. Expression of *mgpA* and *corC* are upregulated under high Mg^{2+} conditions. (A) The *corC* and *mgpA* loci. Dark bars indicate the sequences cloned upstream and in-frame with *lacZ*. The (B) *corC'-'lacZ* and (C) *mgpA'-'lacZ* fusion strains were pre-grown to mid-exponential phase in N-minimal medium pH 7.4 with 1 mM $MgCl_2$ at 37℃, washed, diluted in N-minimal medium pH 5.5, pH 7.4, and pH 8.5 with or without the indicated amount of $MgCl_2$, and incubated at 37℃ for 24h. β-galactosidase activity was measured as described in Materials and Methods section. Values are mean ± SD, n = 6. Paired t test ($p < 0.05$*, 0.005**, 0.0005***) versus 0 mM Mg^{2+} at the same pH. Strains used: JS2734 and JS2735.

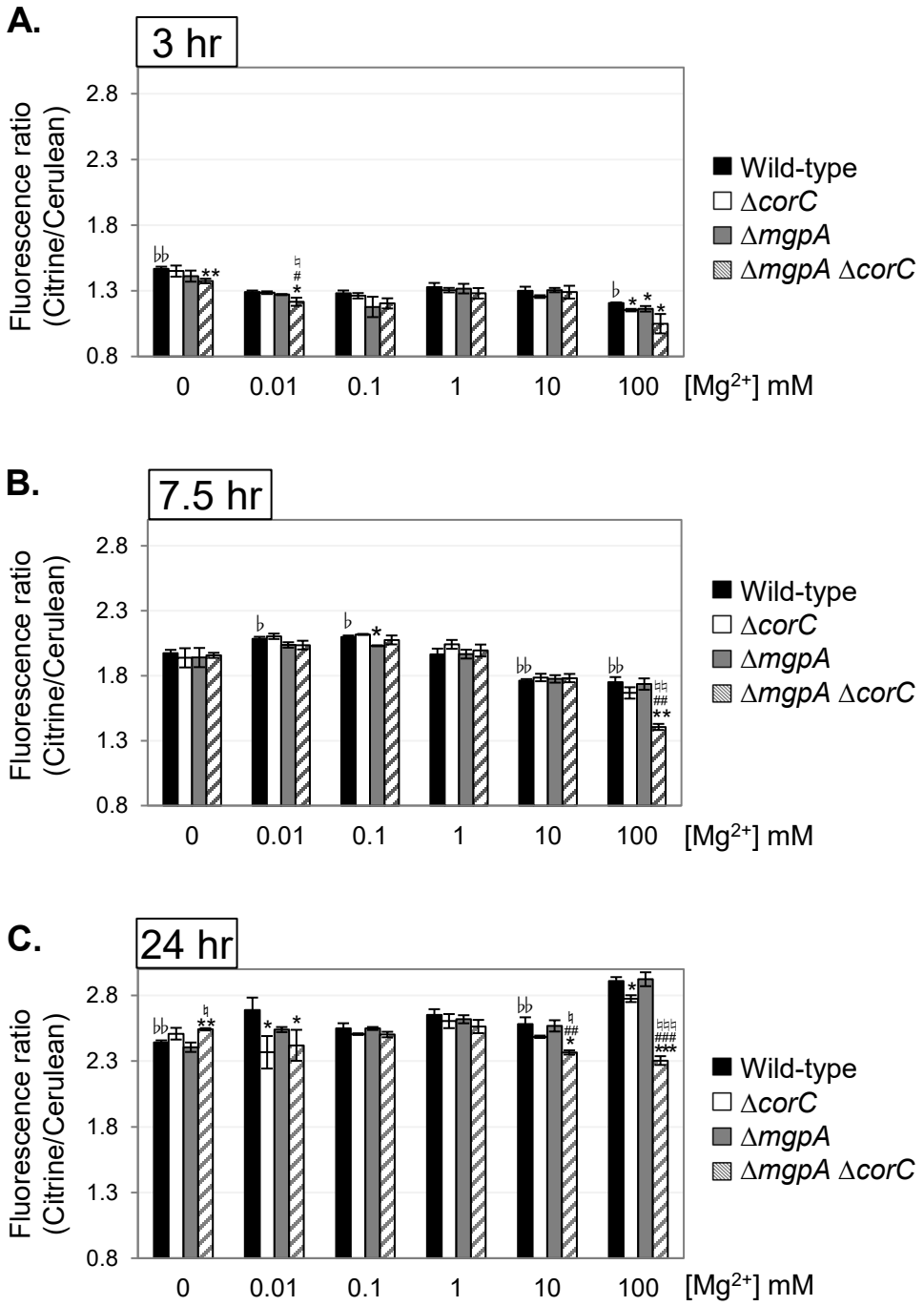

Fig 10. The Δ*corC* strain shows a lower free-Mg level at stationary phase when grown with 100 mM $MgCl_2$, and the deletion of *mgpA* exacerbates the effect. The indicated strains harboring pS2513-MagFRET, pre-grown to mid-exponential phase in N-minimal medium (pH 7.4) with 1 mM $MgCl_2$, were washed and diluted into N-minimal medium pH 7.4 with the indicated amounts of $MgCl_2$, and incubated at 37 ℃. Aliquots (1.5 mL) were collected after (A) 3, (B) 7.5, and (C) 24 hours, and the fluorescence ratio (Citrine/Cerulean) was determined at OD_{600} = 0.1. A higher ratio indicates a higher free-Mg level. Values are mean ± SD, n = 3. Unpaired t test (P < 0.05*; P < 0.005**; P < 0.0005***) versus the wild-type, (P < 0.05#; P < 0.005##; P < 0.0005###) of *mgpA* $^+$ Δ*corC* versus Δ*mgpA* Δ*corC*, or (P < 0.05♮; P < 0.005 ♮♮; P < 0.0005 ♮♮♮) of Δ*mgpA corC* $^+$ versus Δ*mgpA* Δ*corC* at the same condition. Paired t test (P < 0.05 ♭; P < 0.005 ♭♭; P < 0.0005 ♭♭♭) versus 1 mM Mg^{2+} in the wild-type. Strains used: JS2736, JS2737, JS2738, and JS2739.